

VISREASON: A Large-Scale Dataset for Visual Chain-of-Thought Reasoning

Lingxiao Li² Yifan Wang¹ Xinyan Gao³ Chen Tang³ Xiangyu Yue³ Chenyu You^{1†}

¹ Stony Brook University ² Boston University ³ MMLab, CUHK

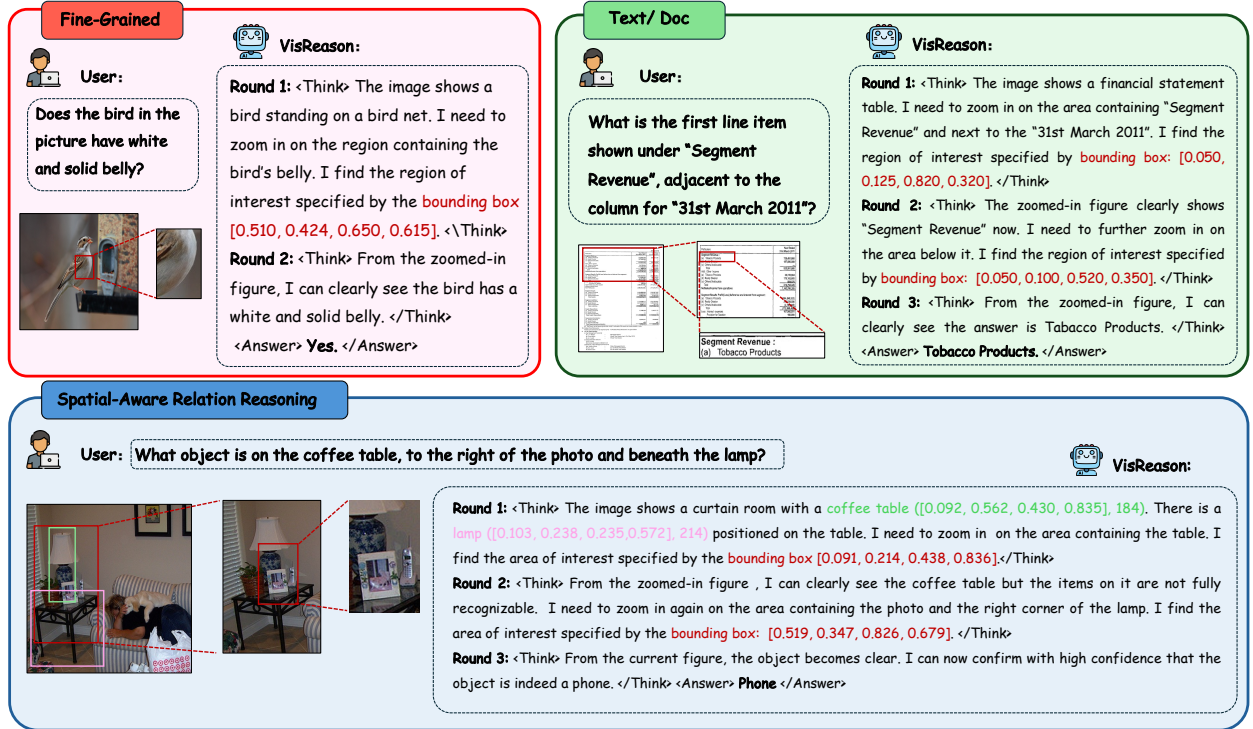


Figure 1. An MLLM fine-tuned on VISREASON emulates a human-like visual reasoning process to solve a complex query. Rather than processing the entire image uniformly, the model adopts a **dynamic global-to-local workflow**: it first assesses the overall scene, then progressively focuses on salient regions to collect fine-grained visual evidence. This multi-step, spatially grounded *visual Chain-of-Thought* allows the model to anchor its reasoning in concrete visual cues, enabling accurate solutions to complex spatial problems that challenge conventional approaches. (Zoom in for better visibility.)

Abstract

Chain-of-Thought (CoT) prompting has proven remarkably effective for eliciting complex reasoning in large language models (LLMs). Yet, its potential in multimodal large language models (MLLMs) remains largely untapped, hindered by the absence of large-scale datasets that capture the rich, spatially grounded reasoning intrinsic to visual understanding. Existing visual-CoT resources are typically small, domain-specific, or lack the human-like stepwise structure

necessary for compositional visual reasoning. In this paper, we introduce VISREASON, a large-scale dataset designed to advance visual Chain-of-Thought reasoning. VisReason comprises 489K annotated examples spanning four diverse domains, each featuring multi-round, human-like rationales that guide MLLMs through interpretable visual reasoning steps. Building upon this, we curate VISREASON-PRO, a 165K subset produced with a stronger expert-level GPT annotator, enriched with detailed reasoning traces and 3D spatial grounding via depth-informed annotations. Fine-tuning the state-of-the-art Qwen2.5-VL model on VisReason and VisReason-Pro yields substantial improvements

[†]Corresponding author.

in step-by-step visual reasoning accuracy, interpretability, and cross-benchmark generalization. These results demonstrate that VisReason equips MLLMs with more systematic and generalizable reasoning capabilities. We envision VisReason as a cornerstone for cultivating human-like visual reasoning, paving the way toward the next generation of multimodal intelligence.

1. Introduction

Recent multimodal large language models (MLLMs) have achieved remarkable progress in practical visual understanding, largely by pairing high-capacity language models with powerful visual encoders through sophisticated alignment pipelines [2, 37, 63, 73]. Foundational models such as LLaVA [29], InternVL [7], Qwen2.5-VL [58], and MiniCPM-V [61], have demonstrated state-of-the-art performance across a wide range of tasks, including visual question answering [23], fine-grained grounding [39], and optical character recognition [69]. These systems have rapidly evolved into versatile visual reasoning assistants for knowledge access, creative work, and embodied interaction.

However, despite architectural advances, the reasoning paradigm of most MLLMs remains rudimentary. In text-only LLMs, Chain-of-Thought (CoT) prompting has revolutionized complex reasoning by training models to articulate explicit intermediate rationales before producing an answer [53]. This stepwise supervision has yielded dramatic improvements in arithmetic, commonsense, and symbolic reasoning. In contrast, the multi-modal domain has yet to experience an equivalent shift [30, 34, 44]. Current MLLMs are predominantly optimized in a direct input-to-answer manner, offering no guidance on intermediate cognitive steps. Although recent work has begun exploring multi-round visual CoTs [41, 47], closely aligned with the broader “thinking-with-images” paradigm [38, 48], these attempts still lack the scale, domain breadth, and spatial grounding necessary to model global-to-local visual reasoning. These deficiencies encourage shortcut learning, over-reliance on linguistic priors, and vulnerability to hallucination when confronted with multi-step visual queries [21].

We argue that this limitation arises from a *fundamental misalignment* between prevailing training paradigms and the structure of human visual cognition. Humans solve visually grounded problems through a global-to-local reasoning process: first forming a holistic hypothesis about the scene, then iteratively narrowing focus to inspect salient regions and refine local evidence. This involves targeted manipulations such as zooming or cropping to probe inter-object relations and depth cues until the task is resolved [41]. While modern VLMs have acquired basic perceptual skills like grounding and OCR during pretraining, they lack supervision that captures this human-like reason-

ing workflow. The root cause is the inadequacy of current visual reasoning datasets, which suffer from three key deficiencies: ❶ limited scale and domain diversity, constraining the ability to learn generalizable reasoning patterns [34, 43, 67]; ❷ insufficient multi-round supervision, often collapsing reasoning into a single-step QA pair without explicit rationales [26, 41, 62]; and ❸ predominantly 2D annotations that neglect depth-aware spatial reasoning crucial for understanding the physical world [43, 44, 56]. This lack of high-quality, cognitively aligned data has become a central obstacle to developing MLLMs capable of genuine visual cognition rather than surface-level perception.

To address these challenges, we introduce VISREASON, a large-scale dataset explicitly designed to instill human-like, spatially grounded reasoning in MLLMs. VISREASON consists of 489K annotated examples across four domains, complemented by VISREASON-PRO, a 165K-example expert-curated subset with richer rationales and depth-informed supervision. To build these, our unified construction pipeline begins by enriching each image with pseudo-3D cues derived from monocular depth estimation and semantic segmentation. Using these 3D-aware scene representations, we prompt advanced MLLMs to generate multi-round visual CoT traces that emulate human reasoning workflows. For VISREASON-PRO, we employ stronger GPT-4.1-series guidance to produce detailed rationales, ensuring higher semantic fidelity and reasoning quality. Each step provides a concise scene summary, identifies a region of interest, and concludes with an explanatory rationale. This fine-grained supervision discourages shortcut learning, promotes global-to-local “zoom-and-verify” behavior, and enhances model generalization. Furthermore, we incorporate explicit 3D grounding – most prominently in VISREASON-PRO – to encourage spatial reasoning directly from single-view depth cues. Building upon this resource, we establish a comprehensive benchmark to evaluate models’ stepwise reasoning and 3D grounding abilities, offering a unified platform for advancing visual CoT research. Our main contributions are as follows:

- We construct and release VISREASON, a large-scale dataset of 489K examples across four diverse domains, together with its 165K high-quality subset VISREASON-PRO produced under stronger GPT-4.1-series guidance. The dataset provides multi-round, human-like step-by-step supervision enriched with depth-informed annotations for advanced spatial reasoning.
- We establish a corresponding benchmark based on VISREASON-PRO, specifically designed to evaluate models’ fine-grained reasoning and 3D grounding capabilities through detailed, multi-step visual CoT tasks.
- We design a unified training and inference pipeline that effectively leverages these annotations to instill sophisticated spatial CoT reasoning in MLLMs. Our models

achieve state-of-the-art performance across multiple metrics, demonstrating improved fidelity, interpretability, and generalizable visual reasoning.

2. Related Works

2.1. Multimodal Large Language Models

The development of multi-modal large language models (MLLMs) has become a central pursuit in advancing existing vision-language research [28, 64]. Contemporary systems typically combine a powerful visual encoder (e.g., ViT [12]) with a projection module, such as an MLP or Q-Former [24], to align visual features with the language embedding space of an LLM for autoregressive decoding [58]. Recent model families, including LLaVA-OneVision [23], InternVL [7], Qwen-VL [2], LLaVA-UHD [57], InternVL-3 [74], Qwen-2.5-VL [3], GPT-4 [37], and Gemini-2.5-Pro [10], have demonstrated remarkable progress in multi-modal reasoning and high-resolution perception. Yet a persistent challenge remains: when visual cues are subtle or spatial relationships are intricate, these models often falter. The prevailing paradigm – processing entire high-resolution images uniformly – limits their ability to allocate computation adaptively. Consequently, models tend to expend capacity on irrelevant regions or depend on superficial linguistic priors rather than engaging in deliberate spatial reasoning. This gap reveals a fundamental misalignment between perceptual capacity and the ability to deploy it strategically for reasoning. Bridging it requires moving beyond monolithic image processing toward adaptive, human-like reasoning workflows – a direction this work aims to advance.

2.2. Multimodal Reasoning

Inspired by the success of Chain-of-Thought (CoT) prompting in enhancing the interpretability and reliability of large language models (LLMs) [15, 53, 66, 71], recent research has sought to instill similar deliberative reasoning in multi-modal large language models (MLLMs). *Model-oriented approaches* aim to elicit such reasoning behavior through in-context learning [8, 14, 16, 36, 49, 70] or via supervised fine-tuning and reinforcement learning [31, 32, 50, 60, 65, 72], enabling MLLMs to generate intermediate rationales without explicit step-level supervision. In parallel, *dataset-oriented efforts* attempt to supervise the reasoning process explicitly, but existing datasets remain limited in both scale and cognitive depth. Concretely, a large portion of prior work simplifies the human reasoning workflow into a single intermediate localization step – representative works include V^* , VPD, Visual CoT, DualFocus, and Chain-of-Spot [4, 18, 30, 44, 54]. Such under-specification often encourages models to learn shortcuts or spurious correlations rather than performing genuine multi-step reasoning. While other datasets introduce multi-round

visual CoTs – a promising step toward more structured reasoning [11, 34, 47, 67, 68] – and relate to the broader “thinking with images” paradigm, they remain constrained by limited scale, narrow domain diversity, and shallow spatial supervision. Moreover, nearly all prior dataset-oriented efforts focus exclusively on 2D grounding, neglecting the depth-aware reasoning required to capture physical spatial relations [43, 44, 56]. In contrast, our work directly addresses these limitations by introducing a large-scale, multi-domain benchmark that provides explicit supervision for multi-round, 3D-aware spatial reasoning, bridging the gap between perception and cognition in MLLMs.

3. VisReason

As detailed in Sec. 1, existing visual reasoning datasets suffer from three persistent limitations – insufficient scale and domain coverage, lack of multi-round stepwise supervision, and minimal depth-aware grounding – necessitating a resource that trains MLLMs to follow human-like visual reasoning. We address these gaps by curating **VISREASON** – a large, spatially aware visual chain-of-thought (CoT) corpus that explicitly supervises the *process* of visual reasoning rather than only final answers. As illustrated in Fig. 2, each sample consists of a question, an answer, and a *multi-round* CoT that mirrors human global-to-local problem solving: every round provides (i) a brief *scene description*, (ii) a predicted *region of interest* (RoI, via bounding box) when zoom is warranted, and (iii) a detailed *rationale* explaining why that RoI suffices. Importantly, zoom-in operations are triggered only when the target object or text is small or visually subtle, allowing the model to retain its efficiency and reliability on simpler cases while engaging in fine-grained reasoning when necessary. Beyond 2D cues, we attach pseudo-3D signals – monocular depth and semantic segmentation – so that the chain can reference ordinal depth and part/region evidence when needed. This unified annotation format encourages models to localize, zoom, and verify iteratively, reducing shortcut learning and promoting depth-aware spatial reasoning.

To ensure broad coverage while keeping the focus on process supervision, **VISREASON** spans *four domains* – text/doc understanding, fine-grained recognition, general VQA, and spatial-aware relational reasoning – continuing and extending prior category choices (Tab. 1). In total, the primary set contains **489k** examples, and we further release a **165k** high-fidelity subset, **VISREASON-PRO**, with richer rationales and stronger depth-informed grounding. Together, these resources offer detailed, stepwise supervision (see Fig. 2) designed to cultivate global-to-local “zoom-and-verify” behaviors and robust reasoning over small objects and complex 2D/3D relations.

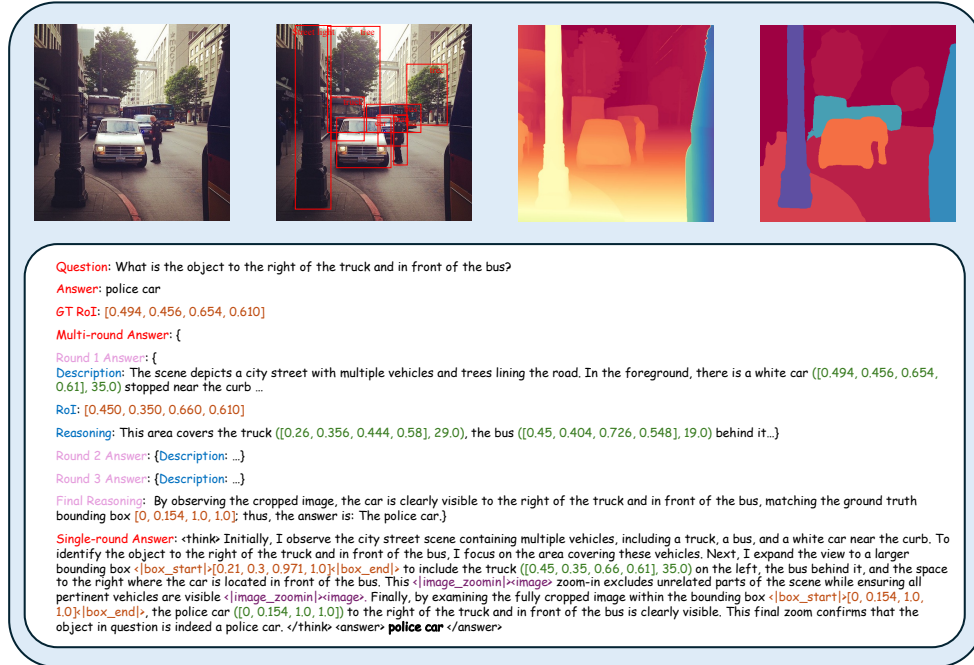


Figure 2. For each image-question pair, we provide a region of interest (bounding box) and a compact multi-round visual chain-of-thought: each round offers a scene sketch, an optional zoom to a predicted RoI, and a brief rationale. When available, depth cues indicate ordinal ordering. The annotations are concise and process-oriented, enabling spatially grounded reasoning on fine details and complex relations.

3.1. Dataset Generation

VISREASON. Building on the Visual-CoT seed [44], we expand each image-question-answer triple with *process-level* supervision. For every example, the model (GPT-4.1-Nano [1]) is prompted to produce a concise scene description, a normalized region of interest (RoI; $[x_1, y_1, x_2, y_2] \in [0, 1]^4$), and a brief rationale. We enforce coverage by adjusting the RoI to tightly contain the ground-truth box and iteratively refining via global-to-local zoom. The refinement terminates when the RoI area is no more than twice the GT area or when a small round budget (≤ 3) is reached. For easier cases where the target object occupies a sufficiently large portion of the image (e.g., $> 30\%$ of the area), we skip iterative cropping and instead provide a single detailed reasoning step followed directly by the final answer. This yields multi-round chains that are compact yet faithful, providing stepwise evidence aligned with the final answer while discouraging shortcut learning.

VISREASON-PRO. As illustrated in Fig. 3, VISREASON-PRO augments the above pipeline with explicit spatial priors to elicit depth-aware reasoning. This subset is constructed primarily from the GQA portion of Visual-CoT, which provides richer annotations (e.g., bounding boxes, relations). We first derive pseudo-3D cues per image – monocular depth and semantic segmentation (object IDs, categories, pixel boxes, and ordinal depths) – and feed these structured signals, together with the image, to a stronger generator

(GPT-4.1-Mini [1]). The model is instructed to create 3D-aware questions whose relations jointly involve 2D layout (*left of, above*) and depth (*in front of, behind*), outputting a consistent GT box for the target. We then apply the same verify-and-fix routine with multi-round zoom (round ≤ 4) to obtain concise descriptions, RoIs, and rationales at each step. In addition to these *multi-round* traces, we provide a *single-round* distilled variant that compacts the multi-step chain into one rationale and a final RoI. As shown in *Single-round Answer* in Fig. 2, our VISREASON-PRO also enables single-pass answering while preserving explicit process supervision. The result is a depth-informed visual CoT corpus tailored for small-object queries and complex 2D/3D relations. More details of the prompt design and algorithms are provided in the Supplementary Material (SM).

3.2. Dataset Analysis

We visualize corpus statistics in Fig. 4 and summarize coverage in Tab. 1. RoIs are strongly biased toward small regions – especially in text/doc tasks – showing that answer-critical evidence often occupies only a minor part of the image ($\sim 13.2\%$ on average), reinforcing the need for models to *localize, zoom, and verify*. Most samples resolve in 2–3 rounds, with harder spatial or 3D cases extending to 4, while easier ones naturally default to a single-step rationale. Notably, the *per-round response length* remains consistently substantial, indicating detailed supervi-

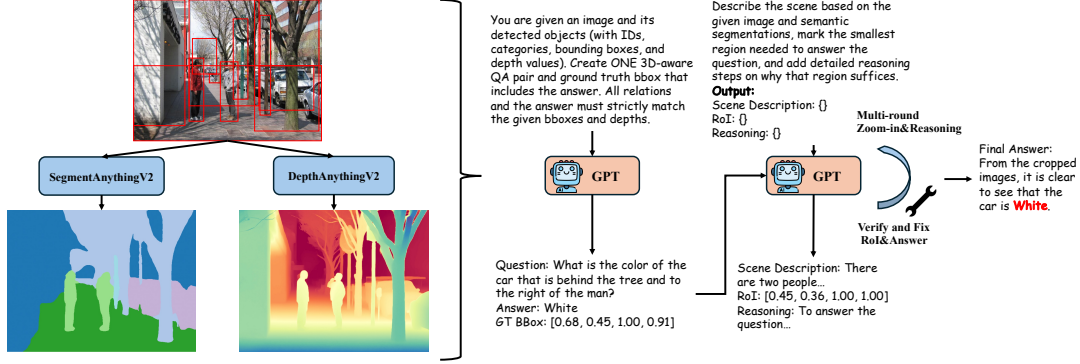


Figure 3. Pipeline for VISREASON and VISREASON-PRO data generation and supervision. Given an input image, we derive semantic segments and monocular depth to form an object list with categories, bounding boxes, and ordinal depth; a generator then produces a 3D-aware QA pair and target box. A second stage emits a compact, multi-round visual CoT – scene sketch, predicted RoI, and rationale – while iteratively zooming and verifying (with RoI/answer fix) until the final answer and finalized annotations are obtained.

sion rather than brief hints and surpassing prior process-level datasets [41, 44, 67]. Overall, VISREASON provides large-scale, explicit multi-round reasoning across diverse domains, complemented by a depth-aware subset (VISREASON-PRO) that strengthens grounded 2D/3D spatial reasoning.

4. Enhancing MLLMs with CoT Reasoning Capabilities

Formulation and Training. Given an image I and textual query Q , our model generates a multi-step reasoning process $Y = (a_0, a_1, \dots, a_T)$ to derive the final answer (Fig. 5). At step t , the action $a_t = (r_t, b_{t+1})$ consists of a textual reasoning snippet r_t and a bounding box b_{t+1} for the next region of interest. Generation is conditioned on prior actions and their visual inputs: the visual context at step t is obtained by cropping I with b_t from the previous step, and we denote features by $\mathcal{V}(\text{crop}(I, b_t))$. The process is initialized with b_0 as the full image. The model auto-regressively outputs the tokens of each a_t – both the rationale and the serialized box coordinates – based on the initial query and the full history of preceding visual and textual data:

$$a_t \sim P_\theta(\cdot | Q, a_0, \dots, a_{t-1}, \mathcal{V}(\text{crop}(I, b_0)), \dots, \mathcal{V}(\text{crop}(I, b_t))). \quad (1)$$

We fine-tune this model on VISREASON via Supervised Fine-Tuning (SFT) using Qwen2.5-VL-7B [3] as the base. During fine-tuning, we apply LoRA [17] for efficient adaptation. The objective maximizes the likelihood of the ground-truth sequence Y given (I, Q) in a standard autoregressive manner, predicting the next token at each step. Concretely, we minimize the negative log-likelihood:

$$\mathcal{L}(\theta) = - \sum_{(I, Q) \in \mathcal{D}} \sum_{t=1}^{|Y|} \log P_\theta(Y_t | I, Q, Y_{<t}), \quad (2)$$

where \mathcal{D} is the training set, θ the trainable parameters, and

Y_t the t -th token of Y . The sequence Y is formed by serializing the multi-step CoT output, converting each b_i into discrete tokens, so the model is trained end-to-end to produce both textual reasoning steps and precise coordinates for focusing visual attention.

5. Experiment

Training Details. We fine-tune Qwen2.5-VL-7B [3] on VISREASON and VISREASON-PRO. The baseline model is first trained for 2 epochs on VISREASON excluding VISREASON-PRO, followed by an additional epoch on the full combined datasets. We adopt a learning rate of 2×10^{-5} for both the LLM backbone and the projector, and 2×10^{-6} for the ViT encoder. Additional training configurations and ablations are provided in the Supplementary Materials.

Benchmarks. We follow the Visual-CoT evaluation protocol [44] and benchmark our models on its 11 source test sets (Fig. 4). As motivated in Sec. 1, we group tasks into four domains: text/document understanding, fine-grained recognition, general VQA, and spatial relational reasoning – to capture both perceptual competence and multi-step spatial inference. To assess robustness beyond these domains, we additionally report results on MME [13] and V*Bench [55], two widely used LVLM evaluation suites covering diverse capabilities and high-resolution visual understanding. For automatic evaluation, we follow prior MLLM work [25, 33, 44] and employ an LLM-based judge to assign a scalar score in the range [0,1] for each example (higher is better). The judging prompt and calibration procedure are provided in the appendix.

5.1. Comparison with State-of-the-art MLLMs

Comparison on Visual-CoT-Benchmark. As shown in Tab. 2, our models achieve the strongest overall performance among open-source MLLMs. VISREASON-PRO-7B obtains the highest average score (0.807), sur-

Domain	Source Dataset	Train/Val Size		GPT Model	Dataset Description
Text/Doc	TextVQA [46]	16k	526	4.1-nano	Images with text
	TextCaps [45]	32k	846	4.1-nano	Images with text
	DocVQA [35]	50k	846	4.1-nano	Doc Images
	DUDE [51]	11k	559	4.1-nano	Doc Images
	SROIE [19]	2k	685	4.1-nano	Invoice Images
Fine-Grained Understanding	Birds-200-2011 [52]	10k	491	4.1-nano	Images of birds
General VQA	Flickr30k [40]	126k	1455	4.1-nano	Images
	Visual7W [75]	30k	994	4.1-nano	Images
Spatial Relatio Reasoning	VSR [27]	3k	404	4.1-nano	Images
	GQA [20] (Pro)	165k	978	4.1-mini	Images (with spatial-aware detailed reasoning steps)
	Open images [22]	43k	944	4.1-nano	Images

Table 1. **Overview of the VisREASON dataset.** It spans four distinct domains and aggregates diverse source datasets, providing broad coverage of visual data styles while supplying spatial-aware, process-level supervision for robust visual chain-of-thought reasoning.

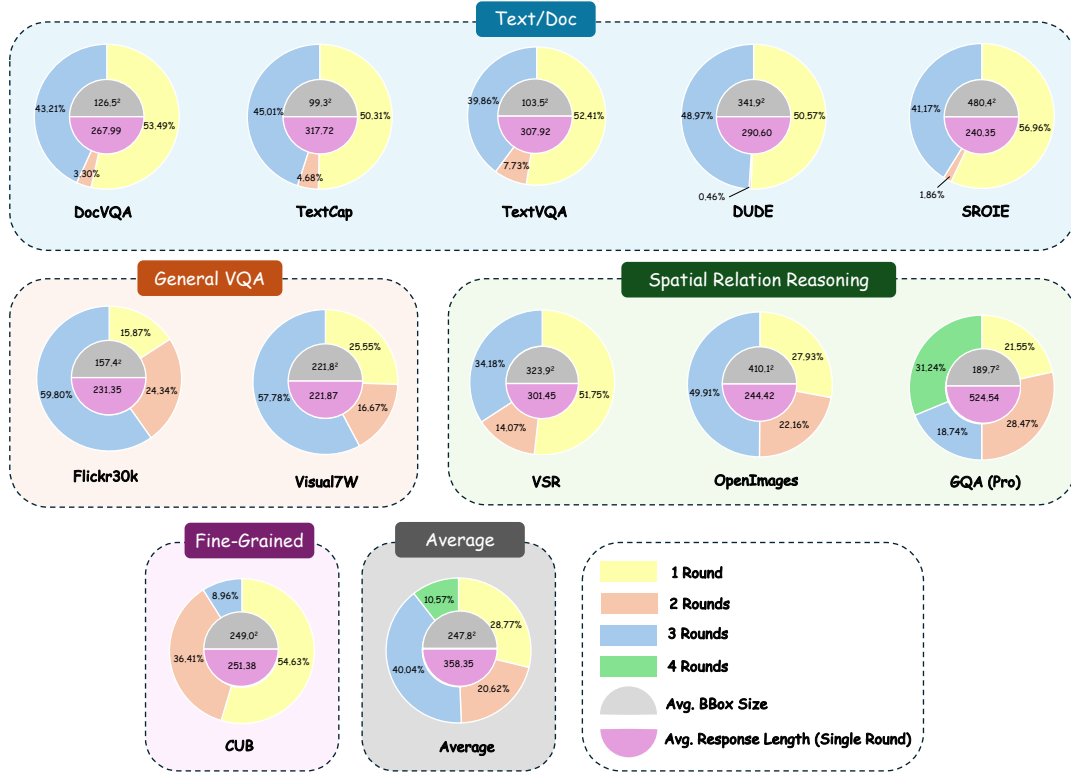


Figure 4. **Statistics of the proposed VisREASON dataset.** We report the distribution of CoT rounds (1–4), the average bounding-box size, and the average response length per round for each source dataset, showing that VisREASON offers rich multi-round supervision and consistently long, detailed reasoning steps across diverse domains.

passing its Qwen-VL-2.5-7B backbone and outperforming InternVL-2.5-8B, LLaVA-NeXT-8B, and VisCoT-7B. These improvements stem from our multi-round, spatially grounded supervision, which provides more reliable localization and stepwise verification than single-step Visual-CoT. Although Qwen-VL-2.5-7B remains slightly better on text/doc OCR tasks, our models retain competitive accuracy while delivering clear gains in fine-grained recogni-

tion, general VQA, and spatial relational reasoning. This small gap is expected, as text regions typically occupy extremely small RoIs, where even minor deviations during zoom-in cropping may exclude the answer tokens. This balanced cross-domain performance indicates that large-scale, depth-aware, multi-round CoT training enhances spatial reasoning without sacrificing the core text understanding ability of the underlying backbone.

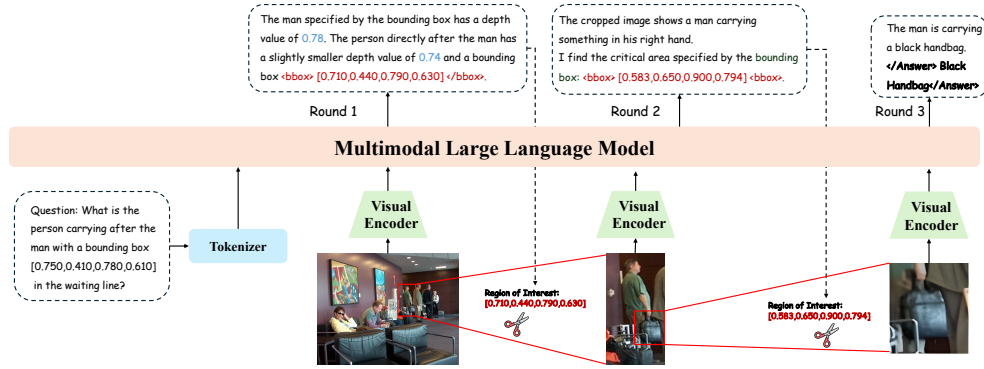


Figure 5. **Overview of VISREASON paradigm.** The model iteratively processes the query by first generating a textual rationale and a bounding box for the next region of interest. It then crops the original image to this region, extracts new visual features, and appends them to the context to inform the next reasoning step, creating a zoom-and-verify sequence.

MLLM	Doc/Text					Fine-grained		General VQA		Spatial Relation Reasoning			Average
	DocVQA	TextCaps	TextVQA	DUDE	SROIE	Birds-200-2011	Flickr30k	Visual7W		GQA	Open Images	VSR	
MiniGPTv2 [5]	0.118	0.378	0.360	0.134	0.01	0.678	0.563	0.635		0.656	0.615	0.626	0.466
VisCoT-7B [44]	0.476	0.675	0.775	0.386	0.470	0.559	0.668	0.558		0.631	0.822	0.614	0.580
LLaVA-NeXT-8B [6]	0.728	0.775	0.850	0.581	0.666	0.715	0.755	0.703		0.736	0.559	0.647	0.705
InternVL-2.5-8B [74]	0.846	0.829	0.907	0.716	0.907	0.747	0.713	0.681		<u>0.689</u>	0.502	0.737	0.738
CoF-SFT-7B [67]	<u>0.955</u>	<u>0.867</u>	<u>0.934</u>	<u>0.813</u>	<u>0.979</u>	0.641	0.606	0.686		0.674	0.503	0.657	0.748
Qwen-VL-2.5-7B [3]	0.964	0.871	0.952	0.817	0.987	0.681	<u>0.772</u>	0.690		0.651	0.498	<u>0.705</u>	0.770
VISREASON-7B	0.926	0.835	0.905	0.778	0.949	<u>0.792</u>	0.766	<u>0.695</u>		0.619	0.798	0.654	<u>0.791</u>
VISREASON-PRO-7B	0.928	0.847	0.922	0.786	0.966	0.831	0.777	0.698		0.670	<u>0.805</u>	0.654	0.807

Table 2. **Comparison with state-of-the-art MLLMs on Visual CoT benchmark.** **Bold** indicates the best results and underline indicates the second best results.

Accuracy	MiniGPTv2	LLaVA-Next	InternVL-2.5	VISREASON	VISREASON-PRO
IoU@0.5 ↑	0.14	0.29	0.08	0.27	0.34
IoU@0.75 ↑	0.06	0.19	0.03	0.13	0.23

Table 3. **Detection performance** on the VISREASON-PRO benchmark. The ground-truth bounding boxes used for computing the metric are the final-round CoT region-of-interest bounding boxes annotated in our VISREASON-PRO benchmark.

	LLaVA-Next	InternVL-2.5	Qwen-VL-2.5	VISREASON-PRO
Grounded Ratio ↑	0.039	0.011	0.035	0.276
BBox (IoU) ↑	0.207	0.214	0.115	0.278
Depth (Abs Diff) ↓	0.394	0.290	0.294	0.266

Table 4. **3D grounding performance** on the VISREASON-PRO benchmark.

Evaluation on the VISREASON-PRO Benchmark The VISREASON-PRO benchmark evaluates two key abilities of spatially grounded reasoning: (i) accurate localization of the predicted RoI and (ii) explicit 3D grounding. RoI accuracy is measured by IoU@0.5/0.75 against the final-round CoT box, with our models using the refined last-round RoI whereas baselines rely on a single-step prediction. 3D grounding is measured through three metrics: the fraction of reasoning steps in which the model proactively grounds the key object it identifies (grounded ratio), the average IoU of these grounded boxes, and the absolute error between the predicted and pseudo-GT ordinal depth. This

setup does not prescribe which objects to ground, making the task a stricter test of whether grounding naturally emerges within the model’s reasoning process.

As shown in Tab. 3 and Tab. 4, our models achieve the highest RoI accuracy, confirming that multi-round zoom-and-verify supervision yields much tighter localization than baselines. VISREASON-PRO also leads by a large margin in 3D grounding, grounding more objects with better box alignment and lower depth error. Although grounded ratios and depth predictions remain challenging for all models, these results show that depth-aware, multi-round supervision substantially improves spatial grounding and produces more faithful reasoning on complex scenes.

Generalization to external benchmarks. As shown in Tab. 5, our models generalize well beyond the Visual-CoT setting, achieving top performance on V* and competitive results on MME. The VISREASON-PRO-7B variant offers strong overall balance, performing favorably against most open-source baselines despite being optimized primarily for spatially grounded CoT. While InternVL-2.5-8B remains stronger on MME – reflecting its broader pretraining coverage – our models exhibit clear advantages on fine-detail following and maintain solid multimodal capability. These results highlight that multi-round, depth-informed supervision not only strengthens spatial reasoning but also transfers effectively to diverse external evaluation suites.

Method	Visual CoT	MME	V*
MiniGPTv2 [5]	0.466	0.752	0.354
VisCoT-7B [44]	0.580	0.701	0.445
LLaVA-NeXT-8B [6]	0.705	0.666	0.597
InternVL-2.5-8B [74]	0.738	0.848	0.597
VisREASON-7B	0.791	0.808	0.619
VisREASON-PRO-7B	0.807	0.777	<u>0.603</u>

Table 5. **Comparison with state-of-the-art MLLMs** on additional benchmarks.

Baseline	Pro	AZ	Doc/Text	General VQA	Relation Reasoning	Fine-grained	Average
✓			0.920	0.739	0.598	0.681	0.770
✓			0.864	0.744	0.678	0.798	0.779
✓	✓	✓	0.882	0.738	<u>0.705</u>	0.792	<u>0.791</u>
✓	✓	✓	0.856	0.750	0.693	<u>0.809</u>	0.781
✓	✓	✓	<u>0.908</u>	<u>0.745</u>	0.729	0.831	0.807

Table 6. **Ablation study** on dataset selection and Zoom-in strategy. (**Baseline** refers to VisREASON, **Pro** refers to VisREASON-PRO, and **AZ** refers to Adaptive Zoom-In Strategy)

Method	AA	GF	SCS	Mean
MiniGPTv2	2.37	1.94	1.88	2.06
VisCoT-7B	2.83	2.58	2.34	2.58
LLaVA-NeXT-8B	3.52	2.93	3.08	3.18
InternVL-2.5-8B	3.87	3.32	3.24	3.48
VisREASON-7B	4.07	4.18	4.12	4.12
VisREASON-PRO-7B	4.19	4.46	4.37	4.34

Table 7. **Human evaluation (1–5)**. AA = Answer Accuracy; GF = Grounded Faithfulness; SCS = Stepwise Clarity & Sufficiency. Mean is an unweighted average across the three criteria.

5.2. Ablation Study

Tab. 6 isolates the contributions of our two dataset variants and the “zoom-in when needed” strategy. Training on VisREASON improves over the Qwen baseline, particularly on relation reasoning and fine-grained tasks, indicating that multi-round spatial supervision provides substantial benefit. Incorporating VisREASON-PRO further strengthens general VQA, relation reasoning, and fine-grained recognition, reflecting the value of higher-fidelity rationales and depth-aware cues. Adding the adaptive zoom-in mechanism yields the best overall performance, boosting fine-grained and relation-heavy benchmarks while largely preserving Doc/Text accuracy. These results confirm that both richer supervision and selective zooming contribute meaningfully to stronger and more balanced visual reasoning.

5.3. User Study

We conducted a blinded study with 30 raters on 20 sampled items per method, evaluating Answer Accuracy (AA), Grounded Faithfulness (GF), and Stepwise Clarity & Sufficiency (SCS). As shown in Tab. 7, models trained on VisREASON achieve clear gains in GF and SCS – reflecting tighter RoIs and more coherent global-to-local chains – which also boosts AA. VisREASON-PRO further

strengthens all three criteria, with raters noting more reliable grounding and more complete reasoning steps. These results confirm that multi-round, depth-aware supervision substantially improves the quality and faithfulness of visual reasoning.

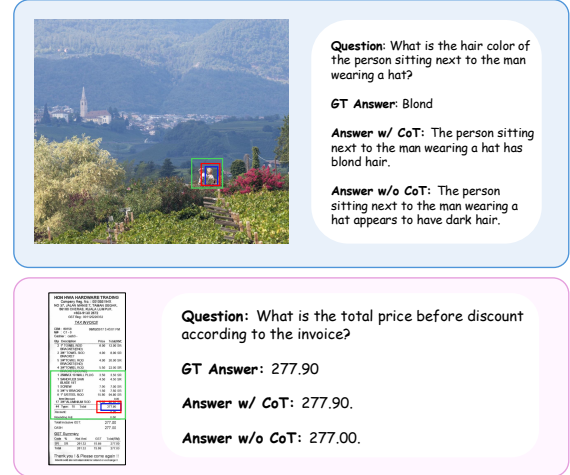


Figure 6. Visualization results of VisREASON to illustrate the difference between various inference modes. Model-generated bounding boxes are shown in green (first-round) and red (second-round), while ground truth (GT) bounding boxes are in blue. Best viewed in color and zoomed in.

5.4. Visualization

Fig. 6 illustrates how our model performs visual CoT reasoning by progressively localizing critical regions and integrating information from both the original and zoomed-in views. We further compare against VisCoT with and without CoT supervision, showing that accurate RoI prediction and coherent stepwise refinement lead to more reliable grounded reasoning and answer quality.

6. Conclusion

In summary, we address key limitations of existing visual CoT – insufficient scale, lack of multi-round supervision, and weak depth awareness – by introducing VisREASON and VisREASON-PRO with compact global-to-local rationales, RoI boxes, and (in VisREASON-PRO) pseudo-3D cues including monocular depth and semantic segmentation. Spanning text/doc, fine-grained, general VQA, and spatial relational tasks, these resources provide rich signals for faithful and spatially grounded inference. Building upon them, we establish a dedicated benchmark for assessing detailed reasoning and 3D grounding. Models trained on the VisREASON series show consistent gains in accuracy, grounded faithfulness, and robustness across diverse evaluations. We hope this dataset family and benchmark offer a strong foundation for advancing spatially aware multimodal reasoning.

References

- [1] Josh Achiam, Steven Adler, Sandhini Agarwal, Lama Ahmad, Ilge Akkaya, Florencia Leoni Aleman, Diogo Almeida, Janko Altenschmidt, Sam Altman, Shyamal Anadkat, et al. Gpt-4 technical report. *arXiv preprint arXiv:2303.08774*, 2023. 4
- [2] Jinze Bai, Shuai Bai, Shusheng Yang, Shijie Wang, Sinan Tan, Peng Wang, Junyang Lin, Chang Zhou, and Jingren Zhou. Qwen-vl: A frontier large vision-language model with versatile abilities. *arXiv preprint arXiv:2308.12966*, 2023. 2, 3
- [3] S. Bai, A. Yang, and Qwen Team. Qwen2.5-vl technical report. *arXiv preprint arXiv:2502.13923*, 2025. 3, 5, 7
- [4] Yuhang Cao, Pan Zhang, Xiaoyi Dong, Dahua Lin, and Jiaqi Wang. Dualfocus: Integrating macro and micro perspectives in multi-modal large language models. *arXiv preprint arXiv:2402.14767*, 2024. 3
- [5] Jun Chen, Deyao Zhu, Xiaoqian Shen, Xiang Li, Zechun Liu, Pengchuan Zhang, Raghuraman Krishnamoorthi, Vikas Chandra, Yunyang Xiong, and Mohamed Elhoseiny. Minigpt-v2: large language model as a unified interface for vision-language multi-task learning. *arXiv preprint arXiv:2310.09478*, 2023. 7, 8
- [6] Lin Chen and Long Xing. Open-llava-next: An open-source implementation of llava-next series for facilitating the large multi-modal model community. <https://github.com/xiaoachen98/Open-LLaVA-NeXT>, 2024. 7, 8
- [7] Zhe Chen, Jiannan Wu, Wenhai Wang, Weijie Su, Guo Chen, Sen Xing, Muyan Zhong, Qinglong Zhang, Xizhou Zhu, Lewei Lu, et al. Internvl: Scaling up vision foundation models and aligning for generic visual-linguistic tasks. In *CVPR*, pages 24185–24198, 2024. 2, 3
- [8] Zhenfang Chen, Qinhong Zhou, Yikang Shen, Yining Hong, Zhiqing Sun, Dan Gutfreund, and Chuang Gan. Visual chain-of-thought prompting for knowledge-based visual reasoning. In *Proceedings of the AAAI Conference on Artificial Intelligence*, pages 1254–1262, 2024. 3
- [9] Bowen Cheng, Alexander Schwing, and Alexander Kirillov. Masked-attention mask transformer for universal image segmentation. In *CVPR*, 2022. 14
- [10] G. Comanici and Gemini Team. Gemini 2.5: Pushing the frontier with advanced reasoning, multimodality, long context, and next-generation agentic capabilities. *arXiv preprint arXiv:2507.06261*, 2025. 3
- [11] Yuhao Dong, Zuyan Liu, Hai-Long Sun, Jingkan Yang, Winston Hu, Yongming Rao, and Ziwei Liu. Insight-v: Exploring long-chain visual reasoning with multimodal large language models. In *CVPR*, 2025. 3
- [12] Alexey Dosovitskiy, Lucas Beyer, Alexander Kolesnikov, Dirk Weissenborn, Xiaohua Zhai, Thomas Unterthiner, Mostafa Dehghani, Matthias Minderer, G Heigold, S Gelly, et al. An image is worth 16x16 words: Transformers for image recognition at scale. In *International Conference on Learning Representations*, 2020. 3
- [13] Chaoyou Fu, Xinyue Yang, Xingyu Chen, Mouxing Sun, Linjiang Qiu, Yi Huang, Yixiao Li, Tianyu Cheng, Jinghao Shi, Zhenyu Xiao, et al. Mme: A comprehensive evaluation benchmark for multimodal large language models. *arXiv preprint arXiv:2306.13394*, 2023. 5
- [14] Zhi Gao, Yuntao Du, Xintong Zhang, Xiaojian Ma, Wenjuan Han, Song-Chun Zhu, and Qing Li. Clova: A closed-loop visual assistant with tool usage and update. In *CVPR*, pages 13258–13268, 2024. 3
- [15] Zhi Gao, Bofei Zhang, Pengxiang Li, Xiaojian Ma, Tao Yuan, Yue Fan, Yuwei Wu, Yunde Jia, Song-Chun Zhu, and Qing Li. Multi-modal agent tuning: Building a vlm-driven agent for efficient tool usage. In *ICLR*, 2025. 3
- [16] Tanmay Gupta and Aniruddha Kembhavi. Visual programming: Compositional visual reasoning without training. In *CVPR*, pages 14953–14962, 2023. 3
- [17] Edward J Hu, Yelong Shen, Phillip Wallis, Zeyuan Allen-Zhu, Yuanzhi Li, Shean Wang, Lu Wang, Weizhu Chen, et al. Lora: Low-rank adaptation of large language models. *ICLR*, 1(2):3, 2022. 5
- [18] Yushi Hu, Otilia Stretcu, Chun-Ta Lu, Krishnamurthy Viswanathan, Kenji Hata, Enming Luo, Ranjay Krishna, and Ariel Fuxman. Visual program distillation: Distilling tools and programmatic reasoning into vision-language models. In *CVPR*, pages 9590–9601, 2024. 3
- [19] Zheng Huang, Kai Chen, Jianhua He, Xiang Bai, Dimosthenis Karatzas, Shijian Lu, and CV Jawahar. Icdar2019 competition on scanned receipt ocr and information extraction. In *2019 International Conference on Document Analysis and Recognition (ICDAR)*, pages 1516–1520. IEEE, 2019. 6
- [20] Drew A Hudson and Christopher D Manning. Gqa: A new dataset for real-world visual reasoning and compositional question answering. In *CVPR*, pages 6700–6709, 2019. 6
- [21] Fucai Ke, Joy Hsu, Zhixi Cai, Zixian Ma, Xin Zheng, Xindi Wu, Sukai Huang, Weiqing Wang, Pari Delir Haghighi, Gholamreza Haffari, Ranjay Krishna, Jiajun Wu, and Hamid Reza Tofighi. Explain before you answer: A survey on compositional visual reasoning. *arXiv preprint arXiv:2508.17298*, 2025. 2
- [22] Alina Kuznetsova, Hassan Rom, Neil Alldrin, Jasper Uijlings, Ivan Krasin, Jordi Pont-Tuset, Shahab Kamali, Stefan Popov, Matteo Mallocci, Alexander Kolesnikov, et al. The open images dataset v4: Unified image classification, object detection, and visual relationship detection at scale. *International Journal of Computer Vision*, 128(7):1956–1981, 2020. 6
- [23] Bo Li, Yuanhan Zhang, Dong Guo, Renrui Zhang, Feng Li, Hao Zhang, Kaichen Zhang, Yanwei Li, Ziwei Liu, and Chunyuan Li. Llava-onevision: Easy visual task transfer. *arXiv preprint arXiv:2408.03326*, 2024. 2, 3
- [24] Junnan Li, Dongxu Li, Silvio Savarese, and Steven Hoi. Blip-2: Bootstrapping language-image pre-training with frozen image encoders and large language models. In *ICML*, pages 19730–19742, 2023. 3
- [25] KunChang Li, Yanan He, Yi Wang, Yizhuo Li, Wenhai Wang, Ping Luo, Yali Wang, Limin Wang, and Yu Qiao. Videochat: Chat-centric video understanding. *arXiv preprint arXiv:2305.06355*, 2023. 5

- [26] Zejun Li, Ruipu Luo, Jiwen Zhang, Minghui Qiu, and Zhongyu Wei. Vocot: Unleashing visually grounded multi-step reasoning in large multi-modal models. *arXiv preprint arXiv:2405.16919*, 2024. 2
- [27] Fangyu Liu, Guy Edward Toh Emerson, and Nigel Collier. Visual spatial reasoning. *Transactions of the Association for Computational Linguistics*, 2023. 6
- [28] Haotian Liu, Chunyuan Li, Qingyang Wu, and Yong Jae Lee. Visual instruction tuning. In *NeurIPS*, 2024. 3
- [29] Shilong Liu, Hao Cheng, Haotian Liu, Hao Zhang, Feng Li, Tianhe Ren, Xueyan Zou, Jianwei Yang, Hang Su, Jun Zhu, et al. Llava-plus: Learning to use tools for creating multi-modal agents. *arXiv preprint arXiv:2311.05437*, 2023. 2
- [30] Zuyan Liu, Yuhao Dong, Yongming Rao, Jie Zhou, and Jiwen Lu. Chain-of-spot: Interactive reasoning improves large vision-language models. *arXiv preprint arXiv:2403.12966*, 2024. 2, 3
- [31] Ziyu Liu, Zeyi Sun, Yuhang Zang, Xiaoyi Dong, Yuhang Cao, Haodong Duan, Dahua Lin, and Jiaqi Wang. Visual-rft: Visual reinforcement fine-tuning. *arXiv preprint arXiv:2503.01785*, 2025. 3
- [32] Zhiyuan Liu, Yuting Zhang, Feng Liu, Changwang Zhang, Ying Sun, and Jun Wang. Othink-mr1: Stimulating multi-modal generalized reasoning capabilities via dynamic reinforcement learning. *arXiv preprint arXiv:2503.16081*, 2025. 3
- [33] Ruipu Luo, Ziwang Zhao, Min Yang, Junwei Dong, Minghui Qiu, Pengcheng Lu, Tao Wang, and Zhongyu Wei. Valley: Video assistant with large language model enhanced ability. *arXiv preprint arXiv:2306.07207*, 2023. 5
- [34] Yunze Man, De-An Huang, Guilin Liu, Shiwei Sheng, Shilong Liu, Liang-Yan Gui, Jan Kautz, Yu-Xiong Wang, and Zhiding Yu. Argus: Vision-centric reasoning with grounded chain-of-thought. In *Proceedings of the IEEE/CVF Conference on Computer Vision and Pattern Recognition (CVPR)*, pages 14268–14280, 2025. 2, 3
- [35] Minesh Mathew, Dimosthenis Karatzas, and CV Jawahar. Docvqa: A dataset for vqa on document images. In *WACV*, pages 2200–2209, 2021. 6
- [36] Chancharik Mitra, Brandon Huang, Trevor Darrell, and Roei Herzig. Compositional chain-of-thought prompting for large multimodal models. In *CVPR*, pages 14420–14431, 2024. 3
- [37] OpenAI. Gpt-4v(ision) system card. 2023. 2, 3
- [38] OpenAI. Thinking with images, 2025. 2
- [39] Zhiliang Peng, Wenhui Wang, Li Dong, Yaru Hao, Shaohan Huang, Shuming Ma, Qixiang Ye, and Furu Wei. Grounding multimodal large language models to the world. In *ICLR*, 2024. 2
- [40] Bryan A Plummer, Liwei Wang, Chris M Cervantes, Juan C Caicedo, Julia Hockenmaier, and Svetlana Lazebnik. Flickr30k entities: Collecting region-to-phrase correspondences for richer image-to-sentence models. In *Proceedings of the IEEE international conference on computer vision*, pages 2641–2649, 2015. 6
- [41] Ji Qi, Ming Ding, Weihang Wang, Yushi Bai, Qingsong Lv, Wenyi Hong, Bin Xu, Lei Hou, Juanzi Li, Yuxiao Dong, et al. Cogcom: Train large vision-language models diving into details through chain of manipulations. *arXiv preprint arXiv:2402.04236*, 2024. 2, 5
- [42] Nikhila Ravi, Valentin Gabeur, Yuan-Ting Hu, Ronghang Hu, Chaitanya Ryali, Tengyu Ma, Haitham Khedr, Roman Rädle, Chloe Rolland, Laura Gustafson, Eric Mintun, Junting Pan, Kalyan Vasudev Alwala, Nicolas Carion, Chao-Yuan Wu, Ross Girshick, Piotr Dollár, and Christoph Feichtenhofer. Sam 2: Segment anything in images and videos. *arXiv preprint arXiv:2408.00714*, 2024. 14
- [43] Gabriel Sarch, Snigdha Saha, Naitik Khandelwal, Ayush Jain, Michael J. Tarr, Aviral Kumar, and Katerina Fragkiadaki. Grounded reinforcement learning for visual reasoning. *arXiv preprint arXiv:2505.23678*, 2025. 2, 3
- [44] Hao Shao, Shengju Qian, Han Xiao, Guanglu Song, Zhuofan Zong, Letian Wang, Yu Liu, and Hongsheng Li. Visual cot: Advancing multi-modal language models with a comprehensive dataset and benchmark for chain-of-thought reasoning. *arXiv preprint arXiv:2403.16999*, 2024. 2, 3, 4, 5, 7, 8, 12
- [45] Oleksii Sidorov, Ronghang Hu, Marcus Rohrbach, and Amanpreet Singh. Textcaps: a dataset for image captioning with reading comprehension. In *ECCV*, pages 742–758. Springer, 2020. 6
- [46] Amanpreet Singh, Vivek Natarajan, Meet Shah, Yu Jiang, Xinlei Chen, Dhruv Batra, Devi Parikh, and Marcus Rohrbach. Towards vqa models that can read. In *Proceedings of the IEEE/CVF conference on computer vision and pattern recognition*, pages 8317–8326, 2019. 6
- [47] Alex Su, Haozhe Wang, Weiming Ren, Fangzhen Lin, and Wenhui Chen. Pixel reasoner: Incentivizing pixel-space reasoning with curiosity-driven reinforcement learning. *arXiv preprint arXiv:2505.15966*, 2025. 2, 3
- [48] Zhaochen Su, Peng Xia, Hangyu Guo, Zhenhua Liu, Yan Ma, Xiaoye Qu, Jiaqi Liu, Yanshu Li, Kaide Zeng, Zhengyuan Yang, et al. Thinking with images for multimodal reasoning: Foundations, methods, and future frontiers. *arXiv preprint arXiv:2506.23918*, 2025. 2
- [49] Shanlin Sun, Gabriel De Araujo, Jiaqi Xu, Shenghan Zhou, Hanwen Zhang, Ziheng Huang, Chenyu You, and Xiaohui Xie. Coma: Compositional human motion generation with multi-modal agents. *arXiv preprint arXiv:2412.07320*, 2024. 3
- [50] Shanlin Sun, Yifan Wang, Hanwen Zhang, Yifeng Xiong, Qin Ren, Ruogu Fang, Xiaohui Xie, and Chenyu You. Ouroboros: Single-step diffusion models for cycle-consistent forward and inverse rendering. In *Proceedings of the IEEE/CVF International Conference on Computer Vision*, pages 10386–10397, 2025. 3
- [51] Jordy Van Landeghem, Rubèn Tito, Łukasz Borchmann, Michał Pietruszka, Paweł Joziak, Rafał Powalski, Dawid Jurkiewicz, Mickaël Coustaty, Bertrand Anckaert, Ernest Valveny, et al. Document understanding dataset and evaluation (dude). In *Proceedings of the IEEE/CVF International Conference on Computer Vision*, pages 19528–19540, 2023. 6
- [52] C. Wah, S. Branson, P. Welinder, P. Perona, and S. Belongie. The caltech-ucsd birds-200-2011 dataset. Technical Report CNS-TR-2011-001, California Institute of Technology, 2011. 6

- [53] Jason Wei, Xuezhi Wang, Dale Schuurmans, Maarten Bosma, Fei Xia, Ed Chi, Quoc V Le, and Denny Zhou. Chain-of-thought prompting elicits reasoning in large language models. In *NeurIPS*, pages 24824–24837, 2022. 2, 3
- [54] Penghao Wu and Saining Xie. v^* : Guided visual search as a core mechanism in multimodal llms. In *CVPR*, pages 13084–13094, 2024. 3
- [55] Pan Wu, Zekai Li, Wenhai Wang, Yuhui Li, Feng Lin, Tong Zhang, Zhaowei Zeng, Kai Zhang, Le Lu, Yu Qiao, and Jifeng Dai. V^* : Guided visual search as a core mechanism in multimodal llms. In *Proceedings of the IEEE/CVF Conference on Computer Vision and Pattern Recognition (CVPR)*, 2024. 5
- [56] Qiong Wu, Xiangcong Yang, Yiyi Zhou, Chenxin Fang, Baiyang Song, Xiaoshuai Sun, and Rongrong Ji. Grounded chain-of-thought for multimodal large language models. *arXiv preprint arXiv:2503.12799*, 2025. 2, 3
- [57] Ruyi Xu, Yuan Yao, Zonghao Guo, Junbo Cui, Zanlin Ni, Chunjiang Ge, Tat-Seng Chua, Zhiyuan Liu, Maosong Sun, and Gao Huang. Llava-uhd: an lmm perceiving any aspect ratio and high-resolution images. *arXiv preprint arXiv:2403.11703*, 2024. 3
- [58] An Yang, Baosong Yang, Beichen Zhang, Binyuan Hui, Bo Zheng, Bowen Yu, Chengyuan Li, Dayiheng Liu, Fei Huang, Haoran Wei, et al. Qwen2. 5 technical report. *arXiv preprint arXiv:2412.15115*, 2024. 2, 3
- [59] Shuwei Yang, Xiaoyu Zhang, Ziyu Wang, and Qi Zhao. Depth anything v2: Unleashing the power of large-scale unlabeled data. *arXiv preprint arXiv:2406.09328*, 2024. 14
- [60] Yi Yang, Xiaoxuan He, Hongkun Pan, Xiyan Jiang, Yan Deng, Xingtao Yang, Haoyu Lu, Dacheng Yin, Fengyun Rao, Minfeng Zhu, et al. R1-onevision: Advancing generalized multimodal reasoning through cross-modal formalization. *arXiv preprint arXiv:2503.10615*, 2025. 3
- [61] Yuan Yao, Tianyu Yu, Ao Zhang, Chongyi Wang, Junbo Cui, Hongji Zhu, Tianchi Cai, Haoyu Li, Weilin Zhao, Zhihui He, et al. Minicpm-v: A gpt-4v level mllm on your phone. *arXiv preprint arXiv:2408.01800*, 2024. 2
- [62] Xubing Ye, Yukang Gan, Xiaoke Huang, Yixiao Ge, Ying Shan, and Yansong Tang. Voco-llama: Towards vision compression with large language models. *arXiv preprint arXiv:2406.12275*, 2024. 2
- [63] Shukang Yin, Chaoyou Fu, Sirui Zhao, Ke Li, Xing Sun, Tong Xu, and Enhong Chen. A survey on multimodal large language models. *arXiv preprint arXiv:2306.13549*, 2023. 2
- [64] Chenyu You, Haocheng Dai, Yifei Min, Jasjeet S Sekhon, Sarang Joshi, and James S Duncan. Uncovering memorization effect in the presence of spurious correlations. *Nature Communications*, 16(1):5424, 2025. 3
- [65] Jingyi Zhang, Jiaying Huang, Huanjin Yao, Shunyu Liu, Xikun Zhang, Shijian Lu, and Dacheng Tao. R1-vl: Learning to reason with multimodal large language models via step-wise group relative policy optimization. *arXiv preprint arXiv:2503.12937*, 2025. 3
- [66] Xiang Zhang, Juntao Cao, Jiaqi Wei, Yiwei Xu, and Chenyu You. Tokenization constraints in llms: A study of symbolic and arithmetic reasoning limits. *arXiv preprint arXiv:2505.14178*, 2025. 3
- [67] Xintong Zhang, Zhi Gao, Bofei Zhang, Pengxiang Li, Xiaowen Zhang, Yang Liu, Tao Yuan, Yuwei Wu, Yunde Jia, Song-Chun Zhu, and Qing Li. Chain-of-focus: Adaptive visual search and zooming for multimodal reasoning via rl. *arXiv preprint arXiv:2505.15436*, 2025. 2, 3, 5, 7
- [68] Xintong Zhang, Zhi Gao, Bofei Zhang, Pengxiang Li, Xiaowen Zhang, Yang Liu, Tao Yuan, Yuwei Wu, Yunde Jia, Song-Chun Zhu, et al. Chain-of-focus: Adaptive visual search and zooming for multimodal reasoning via rl. *arXiv preprint arXiv:2505.15436*, 2025. 3
- [69] Yanzhe Zhang, Ruiyi Zhang, Jiuxiang Gu, Yufan Zhou, Nedim Lipka, Diyi Yang, and Tong Sun. Lllavar: Enhanced visual instruction tuning for text-rich image understanding. *arXiv preprint*, 2023. 2
- [70] Yuechen Zhang, Shengju Qian, Bohao Peng, Shu Liu, and Jiaya Jia. Prompt highlighter: Interactive control for multimodal llms. In *CVPR*, pages 13215–13224, 2024. 3
- [71] Zhuosheng Zhang, Aston Zhang, Mu Li, and Alex Smola. Automatic chain of thought prompting in large language models. *arXiv preprint arXiv:2210.03493*, 2022. 3
- [72] Hengguang Zhou, Xirui Li, Ruochen Wang, Minhao Cheng, Tianyi Zhou, and Cho-Jui Hsieh. R1-zero’s” aha moment” in visual reasoning on a 2b non-sft model. *arXiv preprint arXiv:2503.05132*, 2025. 3
- [73] Deyao Zhu, Jun Chen, Xiaoqian Shen, Xiang Li, and Mohamed Elhoseiny. Minigpt-4: Enhancing vision-language understanding with advanced large language models. *arXiv preprint arXiv:2304.10592*, 2023. 2
- [74] J. Zhu, Z. Chen, W. Wang, et al. Internvl3: Exploring advanced training and test-time strategies for open multimodal models. *arXiv preprint arXiv:2504.10479*, 2025. 3, 7, 8
- [75] Yuke Zhu, Oliver Groth, Michael Bernstein, and Li Fei-Fei. Visual7w: Grounded question answering in images. In *CVPR*, pages 4995–5004, 2016. 6

Supplementary Material

Overview

This appendix is organized as follows:

- Sec. 7: Training configuration and implementation details for VISREASON-7B and VISREASON-PRO-7B.
- Sec. 8: Full data-generation pipelines.
 - Sec. 8.1: Construction of the 2D spatial CoT dataset VISREASON.
 - Sec. 8.2: Construction of the depth-aware dataset VISREASON-PRO.
- Sec. 9: Evaluation protocol on Visual-CoT-Benchmark.
- Sec. 10: Evaluation protocol on VISREASON-PRO.
 - Sec. 10.1: RoI localization evaluation.
 - Sec. 10.2: 3D grounding evaluation.
- Sec. 11: All prompts used in dataset generation, refinement, grounding, and grading.
- Sec. 12: Additional dataset examples.
- Sec. 13: Additional inference examples.

7. Implementation Details

We train both VISREASON-7B and VISREASON-PRO-7B models on a cluster equipped with four NVIDIA H200 GPUs (144 GB memory each). Training is implemented in PyTorch using the HuggingFace LLaMA-Factory framework, with distributed execution based on DeepSpeed ZeRO-2 with CPU offloading. FlashAttention-2 is enabled for efficient attention computation, and KV-cache is disabled to increase training stability. All experiments use bf16 precision.

We adopt LoRA-based parameter-efficient finetuning with a rank of 32 and apply LoRA to all trainable modules. The vision tower of Qwen2.5-VL-7B is frozen throughout training, while the multi-modal projector and language model remain fully trainable. Gradient checkpointing (non-reentrant mode) is activated to reduce memory overhead, allowing a global batch size of 96 on 4 GPUs (per-device batch size $3 \times$ gradient accumulation 4×4 GPUs).

Images are dynamically resized with a minimum of 112×112 pixels (12,544 pixels) and a maximum of 512×512 pixels (262,144 pixels). The maximum sequence length is set to 8,192 tokens, and sample packing is enabled to improve training efficiency. Dataset preprocessing is parallelized using 128 workers, and data loading uses 12 workers per GPU with pinned memory, batch prefetching (factor 6), and persistent worker reuse.

Optimization is performed using the fused AdamW optimizer with a cosine learning rate schedule, a peak learning rate of 1.0×10^{-5} , warmup ratio of 1

All evaluations and ablations are performed on a single

Configuration	VISREASON-7B
Hardware	4× H200 (144 GB)
Precision	bf16
Distributed engine	DeepSpeed ZeRO-2 + CPU offload
Flash attention	FlashAttention-2
LoRA rank	32 (all trainable modules)
Frozen modules	Vision tower only
Dataset / Input	
Dataset Use	VISREASON
Cutoff length (tokens)	8192
Image max pixels	262,144 (512×512)
Image min pixels	12,544 (112×112)
Packing	Enabled
Training	
Base model	Qwen2.5-VL-7B-Instruct
Global batch size	96
Per-device batch size	3
Gradient accumulation	4
Epochs	2
Optimizer	AdamW (fused)
Learning rate	1.0×10^{-5}
Scheduler	Cosine, warmup 1%
Gradient clipping	1.0
Gradient checkpointing	Enabled (non-reentrant)
Use cache (KV)	Disabled
Group-by-length	Enabled
Drop last batch	True
Dataloader	
Preprocessing workers	128
Dataloader workers	$12 \times 4 = 48$
Pin memory	True
Prefetch factor	6
Persistent workers	True
Saving	
Save every steps	50
Max checkpoints	3
Format	safetensors

Table 8. Detailed training configuration for VISREASON.

NVIDIA A800 GPU (80 GB memory) under bf16 precision.

Tab. 8 and Tab. 9 summarize the main hyperparameters used for VISREASON-7B and VISREASON-PRO-7B, respectively.

8. Data Generation Details

8.1. Construction of the VISREASON Dataset

VISREASON is derived from the *regular* portion of the Visual-CoT dataset [44]. The original split provides, for each sample, an image, a natural-language question, a short answer, a long-form explanation, and a set of object annotations with semantic labels and xywh-formatted bounding boxes. However, the regular split does not contain

Configuration	VISREASON-PRO-7B
Hardware	4× H200 (144 GB)
Precision	bf16
Distributed engine	DeepSpeed ZeRO-2 + CPU offload
Flash attention	FlashAttention-2
LoRA rank	32 (all trainable modules)
Frozen modules	Vision tower only
Dataset / Input	
Dataset Use	VISREASON-PRO
Cutoff length (tokens)	8192
Image max pixels	262,144 (512 × 512)
Image min pixels	12,544 (112 × 112)
Packing	Enabled
Training	
Base model	VISREASON-7B
Global batch size	96
Per-device batch size	3
Gradient accumulation	4
Epochs	1
Optimizer	AdamW (fused)
Learning rate	1.0×10^{-5}
Scheduler	Cosine, warmup 1%
Gradient clipping	1.0
Gradient checkpointing	Enabled (non-reentrant)
Use cache (KV)	Disabled
Group-by-length	Enabled
Drop last batch	True
Dataloader	
Preprocessing workers	128
Dataloader workers	$12 \times 4 = 48$
Pin memory	True
Prefetch factor	6
Persistent workers	True
Saving	
Save every steps	50
Max checkpoints	3
Format	safetensors

Table 9. Detailed training configuration for VISREASON-PRO.

any process-level reasoning, intermediate region-of-interest (RoI) annotations, or multi-step spatial justification. To obtain explicit spatial chain-of-thought (CoT) supervision, we enrich every sample with multi-round descriptions, rationales, and refined RoIs.

Round-1 expansion. For each image–QA pair, we first perform a single-round expansion that prompts a vision–language model (VLM) with the full-resolution image, the question, and the short answer. The model returns three components: (i) a compact description of the scene, (ii) a normalized RoI $\hat{A}_1 \in [0, 1]^4$, and (iii) a brief rationale that justifies the predicted region. We convert \hat{A}_1 to pixel coordinates and apply an adjustment operation that guarantees

coverage of the ground-truth bounding box B^* while respecting image boundaries.

Multi-round iterative refinement. To capture finer spatial relations, we apply an adaptive multi-round zoom-in strategy. After Round 1, if the predicted RoI remains significantly larger than the GT box (i.e., $\text{Region}(A_t) > N \cdot \text{Region}(B^*)$), we crop the current RoI from the image and prompt the VLM again using only the cropped region. The model produces a new triplet $(\text{desc}_{t+1}, \hat{A}_{t+1}, \text{reason}_{t+1})$, where \hat{A}_{t+1} is predicted in local coordinates. This box is mapped back to the global system, adjusted to cover B^* , and used as the basis for the next iteration. The refinement continues for at most $R_{\max} = 3$ rounds or until the region ratio constraint is satisfied.

Final justification. After the refinement terminates, the last cropped view is used to obtain a single-sentence final justification explicitly referencing the GT object. All intermediate results are stored as a multi-round chain:

$$\{(\text{desc}_t, A_t, \text{reason}_t)\}_{t=1}^T.$$

This chain reflects a progressively localized reasoning process aligned with the final answer.

Optional consistency enhancement. To improve annotation quality, we perform an additional refinement pass that validates bounding boxes across rounds, corrects out-of-bound predictions, removes implausible RoIs, and ensures consistent local-to-global coordinate transformations. This results in more stable multi-round traces, especially in complex or cluttered scenes.

Final output. Each VISREASON sample contains scene descriptions, rationales, and refined RoIs at every round, together with a final justification. The result is a large-scale 2D spatial CoT dataset derived from Visual-CoT, providing explicit stepwise grounding signals for training multimodal reasoning models.

8.2. Construction of the VISREASON-PRO Dataset

VISREASON-PRO builds upon the GQA-derived portion of Visual-CoT, which contains richer annotations than the regular split, including object categories, object-level bounding boxes, and fine-grained relational metadata. Nevertheless, these annotations remain purely 2D: neither GQA nor Visual-CoT provide depth maps, ordinal depth relationships, or 3D-aware QA pairs. VISREASON-PRO augments this data with pseudo-3D cues and depth-sensitive spatial CoT traces.

Pseudo-3D annotation. To obtain depth- and geometry-aware signals for VISREASON-PRO, each GQA image is augmented with both monocular depth and semantic segmentation derived from strong foundation models. Depth is estimated using *Depth-Anything V2* [59], a state-of-the-art transformer-based monocular depth estimator that produces a dense depth field $D \in [0, 1]^{H \times W}$ after min-max normalization. In parallel, we compute instance-level semantic segmentation using the *Mask2Former* universal segmentation model [9], based on a Swin-L large backbone, which yields per-pixel semantic labels and multi-object instance masks.

To further improve spatial consistency, especially for small or fragmented regions, we perform depth-guided region merging: small connected components in the semantic map are merged into adjacent regions whose mean depth differs by less than a threshold (0.15), ensuring geometrically coherent segmentation. In addition, object-level masks are refined using SAM2 [42], from which high-quality binary masks are obtained for all sufficiently large objects.

For each detected object, we compute: (i) a segmentation-aligned bounding box, (ii) the robust depth estimate (median depth over the mask, corrected by depth statistics at anchor points), and (iii) an ordinal depth ranking among all objects in the image. This yields a structured object list

$$\mathcal{O} = \{(c_i, [x_1, y_1, x_2, y_2]_i, d_i)\}_{i=1}^K,$$

where c_i denotes the semantic category, and d_i is the object’s ordinal depth in the global scene order. These pseudo-3D cues enable our generator to compose questions involving coupled 2D and depth relations (*left of*, *above*, *in front of*, *behind*), and support multi-round 3D-grounded reasoning in VISREASON-PRO.

3D-aware QA generation. To introduce depth reasoning, we instruct a VLM to generate new QA pairs that jointly involve 2D spatial relations (*left of*, *above*) and depth relations (*in front of*, *behind*). The model receives the image and the enriched object list \mathcal{O} and produces a depth-aware question, a short answer, a long answer, and a GT bounding box for the referenced target object. The output is converted into pixel coordinates and normalized to match the style of the Visual-CoT annotations. This stage produces 3D-aware samples tightly aligned with the geometric structure of the scene.

Multi-round 3D-aware CoT refinement. We construct depth-sensitive multi-round CoT traces using a refinement process similar to the VISREASON pipeline but extended to incorporate 3D cues. At each round, the prompt includes the

cropped image region and the subset of objects whose boxes fall inside the crop. Their depth values are re-normalized locally, ensuring that ordinal ordering remains consistent under cropping. The VLM predicts a description, a local RoI, and a rationale that may reference both spatial and depth relations. The predicted box is mapped back to global coordinates, adjusted to ensure coverage of the GT box, and passed to the next round. This refinement proceeds for up to $R_{\max} = 4$ rounds or until the region ratio constraint is satisfied.

Grounding-aware rationale augmentation. To maintain alignment between textual reasoning and pixel evidence, we optionally augment the model-generated rationales by explicitly mentioning object identities, bounding boxes, and ordinal depths when they appear in the reasoning. This produces richer supervision signals that couple linguistic explanations with spatial and depth structure.

Final output. Each VISREASON-PRO entry contains: (i) a depth-sensitive question, (ii) the short and long answers, (iii) an object list with segmentation-derived bounding boxes and ordinal depths, and (iv) a multi-round chain of $(desc_t, A_t, reason_t)$ triplets. A distilled single-round variant is also provided, compressing the entire CoT trajectory into one step. The resulting dataset forms a high-fidelity 2D–3D spatial reasoning corpus suitable for evaluating depth-aware multimodal models.

Algorithm 1 VISREASON: Multi-round 2D Spatial CoT Generation

Require: Image I , question q , short answer a , GT box B^* ; max rounds $R_{\max}=3$; area ratio threshold $N=2$; large-object threshold τ_{large} ; generator \mathcal{G}

Ensure: Multi-round chain $\{(\text{desc}_t, \text{RoI}_t, \text{reason}_t)\}_{t=1}^T$ and a final justification

- 1: $(W, H) \leftarrow \text{size}(I)$
- 2: Compute image area $A_{\text{img}} \leftarrow W \cdot H$ and GT area $A_{\text{GT}} \leftarrow \text{Region}(B^*)$
- 3: **if** $A_{\text{GT}}/A_{\text{img}} \geq \tau_{\text{large}}$ **then**
- 4: Prompt \mathcal{G} with (I, q, a) to obtain $\text{desc}_1, \hat{A}_1 \in [0, 1]^4, \text{reason}_1$
- 5: $A_1 \leftarrow \text{ratio2xyxy}(\hat{A}_1; W, H)$
- 6: $A_1 \leftarrow \text{ADJUSTROI}(A_1, B^*)$
- 7: Query \mathcal{G} with (I, q, a, B^*) for a one-sentence final justification
- 8: **return** $\{(\text{desc}_1, A_1, \text{reason}_1)\}$ and final justification
- 9:
- 10: $t \leftarrow 1$
- 11: **(Round 1)** Prompt \mathcal{G} with (I, q, a) to obtain $\text{desc}_1, \hat{A}_1 \in [0, 1]^4, \text{reason}_1$
- 12: $A_1 \leftarrow \text{ratio2xyxy}(\hat{A}_1; W, H)$
- 13: $A_1 \leftarrow \text{ADJUSTROI}(A_1, B^*)$ \triangleright ensure GT coverage and in-bounds
- 14: **while** $t < R_{\max}$ **and** $\text{Region}(A_t) > N \cdot \text{Region}(B^*)$ **do**
- 15: $I_{t+1} \leftarrow \text{crop}(I, A_t)$
- 16: Prompt \mathcal{G} with (I_{t+1}, q, a) to obtain $\text{desc}_{t+1}, \hat{A}_{t+1}, \text{reason}_{t+1}$
- 17: Map local box to global coords: $A_{t+1} \leftarrow \text{local2global}(\hat{A}_{t+1}; A_t)$
- 18: $A_{t+1} \leftarrow \text{ADJUSTROI}(A_{t+1}, B^*)$
- 19: $t \leftarrow t + 1$
- 20: $T \leftarrow t; A_{\text{final}} \leftarrow A_T; I_{\text{final}} \leftarrow \text{crop}(I, A_{\text{final}})$
- 21: Query \mathcal{G} once more with $(I_{\text{final}}, q, a, B^*)$ for a one-sentence final justification
- 22: Optionally run a consistency check to correct out-of-bound or implausible boxes across $\{A_t\}_{t=1}^T$
- 23: **return** $\{(\text{desc}_t, A_t, \text{reason}_t)\}_{t=1}^T$ and final justification
- 24: **function** $\text{ADJUSTROI}(A, B^*)$
- 25: $A \leftarrow A \cup B^*$ \triangleright expand to include the GT box
- 26: $A \leftarrow \text{clipToImage}(A)$
- 27: **return** A

Algorithm 2 VISREASON-PRO: Depth-aware Spatial CoT Generation

Require: Image I ; optional seed QA (q_0, a_0, B_0^*) ; max rounds $R_{\max}=4$; area ratio threshold $N=2$; large-object threshold τ_{large} ; QA generator \mathcal{G}_Q ; CoT generator \mathcal{G}_{CoT}

Ensure: 3D-aware QA (q, a, B^*) and multi-round chain $\{(\text{desc}_t, \text{AoI}_t, \text{reason}_t)\}_{t=1}^T$

- 1: **(Pseudo-3D annotation)**
- 2: $D \leftarrow \text{MonocularDepth}(I)$ \triangleright dense normalized depth map
- 3: $S \leftarrow \text{Seg}(I)$ \triangleright instance-level semantic segmentation
- 4: Build object list $\mathcal{O} = \{(c_i, [x_1, y_1, x_2, y_2]_i, d_i)\}_{i=1}^K$ from (S, D)
- 5: \triangleright bounding box, category, and ordinal depth d_i for each object
- 6:
- 7: **if** no seed QA is provided **then**
- 8: $(q, a, B^*) \leftarrow \mathcal{G}_Q(I, \mathcal{O})$
- 9: \triangleright generate 3D-aware QA with 2D (*left of, above*) + depth (*in front of, behind*) relations
- 10: **else**
- 11: $(q, a, B^*) \leftarrow (q_0, a_0, B_0^*)$
- 12:
- 13: $(W, H) \leftarrow \text{size}(I)$
- 14: Compute image area $A_{\text{img}} \leftarrow W \cdot H$ and GT area $A_{\text{GT}} \leftarrow \text{Region}(B^*)$
- 15: **if** $A_{\text{GT}}/A_{\text{img}} \geq \tau_{\text{large}}$ **then**
- 16: Prompt \mathcal{G}_{CoT} with (I, q, a, \mathcal{O}) to obtain $\text{desc}_1, \hat{A}_1, \text{reason}_1$
- 17: $A_1 \leftarrow \text{ratio2xyxy}(\hat{A}_1; W, H)$
- 18: $A_1 \leftarrow \text{ADJUSTAOI}(A_1, B^*)$
- 19: Optionally distill a single-round rationale from $(\text{desc}_1, \text{reason}_1)$
- 20: **return** (q, a, B^*) and $\{(\text{desc}_1, A_1, \text{reason}_1)\}$
- 21:
- 22: $t \leftarrow 1$
- 23: **(Round 1)** Prompt \mathcal{G}_{CoT} with (I, q, a, \mathcal{O}) to obtain $\text{desc}_1, \hat{A}_1, \text{reason}_1$
- 24: $A_1 \leftarrow \text{ratio2xyxy}(\hat{A}_1; W, H)$
- 25: $A_1 \leftarrow \text{ADJUSTAOI}(A_1, B^*)$
- 26: **while** $t < R_{\max}$ **and** $\text{Region}(A_t) > N \cdot \text{Region}(B^*)$ **do**
- 27: $I_{t+1} \leftarrow \text{crop}(I, A_t)$
- 28: Extract local object subset $\mathcal{O}_{t+1} \subseteq \mathcal{O}$ whose boxes intersect A_t
- 29: Re-normalize depths in \mathcal{O}_{t+1} to local ordinal ranks
- 30: Prompt \mathcal{G}_{CoT} with $(I_{t+1}, q, a, \mathcal{O}_{t+1})$ to obtain $\text{desc}_{t+1}, \hat{A}_{t+1}, \text{reason}_{t+1}$
- 31: $\text{desc}_{t+1}, \hat{A}_{t+1}, \text{reason}_{t+1}$
- 32: Map local box to global coords: $A_{t+1} \leftarrow \text{local2global}(\hat{A}_{t+1}; A_t)$
- 33: $A_{t+1} \leftarrow \text{ADJUSTAOI}(A_{t+1}, B^*)$
- 34: $t \leftarrow t + 1$
- 35: $T \leftarrow t$
- 36: Optionally distill a single-round rationale from $\{(\text{desc}_t, A_t, \text{reason}_t)\}_{t=1}^T$
- 37: **return** (q, a, B^*) and $\{(\text{desc}_t, A_t, \text{reason}_t)\}_{t=1}^T$
- 38: **function** $\text{ADJUSTAOI}(A, B^*)$
- 39: $A \leftarrow A \cup B^*$ \triangleright enforce GT coverage
- 40: $A \leftarrow \text{clipToImage}(A)$
- 41: **return** A

9. Evaluation Protocol on Visual-CoT-Benchmark

To support the comparisons in Sec. 5.1 in the main paper, we describe here the exact evaluation protocol used on Visual-CoT-Benchmark.

Multi-round zoom-in evaluation. To mirror the training-time multi-round spatial CoT supervision, we evaluate models with an explicit *zoom tool* that the model can call when necessary. The tool takes a ratio-based bounding box $\text{bbox}_2=[x_1, y_1, x_2, y_2] \in [0, 1]^4$ on the *current* view and returns a cropped image patch. Before cropping, we validate the box (all coordinates in $[0, 1]$, $x_1 < x_2$, $y_1 < y_2$); invalid proposals are discarded and the model continues on the previous view. A valid box is mapped to absolute pixel coordinates on the parent view, clipped to the image boundaries, and used to crop the next view. The crop is optionally upsampled (while preserving aspect ratio) to keep its pixel count within the same budget as the global view, and this new patch becomes the input image for the next round.

The dialog protocol is as follows. In the first round, the user message consists of the resized global image and a textual query: we instruct the model to (i) think before answering, and (ii) either answer directly or request a zoom if the current view is insufficient (small text, heavy clutter, multiple candidates, etc.). If the model decides to zoom, we apply the crop described above, attach the cropped image as the new visual input, and append a short textual instruction indicating that this is a zoomed-in view; the model is again asked to think and decide whether another zoom is needed. This process repeats for at most $R_{\max}=5$ rounds per example. As soon as the model produces a final answer (without requesting further zooms), the interaction stops and that answer is recorded. Empirically, most examples terminate within 2–3 rounds.

Answer extraction and dataset handling. For each completed interaction, we parse the model output to extract the final natural language answer string. The prompt format explicitly asks the model to wrap its prediction into a dedicated answer segment, but our extractor is robust: if the expected markup is missing, we fall back to the raw text after minimal trimming. For each constituent dataset in Visual-CoT-Benchmark (e.g., CUB, TextVQA, DocVQA, GQA and others), we follow the official validation splits and JSON annotations provided by the benchmark authors. Each entry specifies the image path, the question, and the ground-truth answer (or option letter for multiple-choice questions). For datasets where the original evaluation protocol includes answer normalization (e.g., case folding, punctuation stripping, synonym mapping), we apply the same normalization as the official scripts; we then compute accuracy as the fraction of examples where the normalized prediction matches the normalized ground truth.

Aggregating metrics. Per-dataset accuracies are computed independently and then macro-averaged across all Visual-CoT-Benchmark subsets to obtain the “Avg.” scores reported in Tab. 2 in the main paper. All baseline results are either taken from the original Visual-CoT-Benchmark paper or reproduced using the same protocol, ensuring that our VISREASON-7B and VISREASON-PRO-7B numbers are directly comparable to prior MLLMs under an identical evaluation setup.

10. Evaluation Protocol on the VISREASON-PRO Benchmark

10.1. Region-of-Interest Localization Evaluation

For the RoI localization metrics in Tab. 3 in the main paper, we evaluate all models under a unified multi-round zoom-answer interface that mimics the VISREASON-PRO data-generation pipeline.

Multi-round interaction interface. Given an image I , a question q , and its ground-truth target box B^* , the model is queried in a chat-style interface with tool support. The system prompt exposes a single image *zoom* tool whose argument is a ratio-based bounding box $\text{bbox}_2=[x_1, y_1, x_2, y_2] \in [0, 1]^4$ on the *current* view. At each round, the model must always produce a private reasoning segment enclosed in `<think>...</think>`. It can then either: (i) call the zoom tool once via a `<tool_call>` tag, or (ii) output the final answer via an `<answer>` tag. The prompt strictly forbids mixing `<tool_call>` and `<answer>` in the same round, ensuring a clean separation between “zoom” and “answer” steps. We cap the total number of rounds by a small constant R_{\max} (typically $R_{\max}=6$).

Zoom execution and box propagation. Whenever the model emits a `<tool_call>`, we parse the JSON arguments, validate the predicted ratio box (four numeric coordinates, all in $[0, 1]$, with $x_1 < x_2$, $y_1 < y_2$), and map it to absolute pixel coordinates on the current view. The resulting box is clipped to the image boundaries and used to crop the next view; the crop is resized to satisfy a fixed pixel budget while preserving aspect ratio, and encoded back into the next-round prompt as an image. This process is repeated until either the model chooses to answer (emits `<answer>`) or the round budget R_{\max} is reached. Any malformed or out-of-range box proposals are discarded and the model continues with the previous view, which prevents pathological tool calls from corrupting the evaluation.

Predicted RoI extraction. For models trained with multi-round spatial supervision (our VISREASON-PRO-7B and VISREASON-7B), the final predicted RoI is taken to be the last valid zoom box produced in the interaction, i.e., the box that defines the final view when the answer is given. For single-step baselines that do not explicitly emit zoom

calls, the prompt instructs them to directly produce a single ratio-based box in their first (and only) reasoning step, which is then treated as their predicted RoI. In both cases, the predicted box is represented in the global image coordinate system to allow direct comparison with B^* .

Localization metrics. Given the predicted box \hat{B} and the ground-truth box B^* , we compute the intersection-over-union score

$$\text{IoU}(\hat{B}, B^*) = \frac{\text{Area}(\hat{B} \cap B^*)}{\text{Area}(\hat{B} \cup B^*)}.$$

RoI accuracy is then reported as the fraction of examples whose IoU exceeds standard thresholds, i.e., $\text{IoU}@0.5$ and $\text{IoU}@0.75$. Our models use the refined last-round box \hat{B}_T after multi-round zoom-and-verify, whereas baselines rely on their single-step prediction, making improvements attributable to our iterative cropping strategy rather than differences in IoU computation.

10.2. 3D Grounding Evaluation

For the 3D grounding metrics in Tab. 4 in the main paper, we evaluate whether models can *explicitly* annotate key objects with consistent 2D boxes and ordinal depth in their reasoning traces.

Reasoning-format constraints. Each evaluation example consists of an image I , a question q , and pseudo-3D annotations from VISREASON-PRO, which include a set of key objects with ground-truth ratio boxes and normalized depths. At inference time, the system prompt requires every model to write, *inside* its `<think>` segment, a list of spatial annotations of the form

$$\text{name} : ([x_1, y_1, x_2, y_2], \text{depth}),$$

for all salient or answer-relevant objects. The box coordinates must be ratio-based and lie in $[0, 1]$, while the depth is also constrained to $[0, 1]$ (interpreted as a discrete ordinal depth from the current viewpoint). The model is free to choose object names, but is explicitly encouraged to annotate the objects it relies on to answer the question. No additional crops are allowed in this protocol; we focus purely on the quality of grounding expressed in the reasoning itself.

Parsing predicted groundings. From the generated `<think>` segment, we parse all entries matching the pattern

$$\text{name} : ([x_1, y_1, x_2, y_2], d),$$

using a robust regular expression that tolerates different separators, whitespace, and minor formatting variations. The parser supports: (i) boxes given directly as ratios; (ii) boxes given in percentages (automatically divided by 100); and (iii) boxes given in pixels (optionally normalized using the image width and height, when available). All boxes are clipped to $[0, 1]^4$ and corrected to ensure $x_1 < x_2, y_1 < y_2$.

Depth values d can be numeric or symbolic; numeric depths are normalized to $[0, 1]$, while symbolic depths such as “near”, “mid(dle)”, and “far” are mapped to fixed ordinal levels (e.g., 0.2, 0.5, 0.8). The result is, for each model, a dictionary of predicted objects with fields `bbbox_ratio` and `depth01`.

Ground-truth object set. On the dataset side, VISREASON-PRO provides, for each reasoning step, the key objects that should be grounded in order to support the answer, along with their ratio boxes and normalized depths. For the analysis in Tab. 4 in the main paper, we focus on the first reasoning step (which is shared across all models) and extract the ground-truth object set by parsing the reference description and rationale with the same grounding parser, yielding a dictionary of ground-truth objects with `bbbox_ratio` and `depth01` fields.

Matching and metrics. For each example, we align predicted and ground-truth objects by their textual names (after lowercasing). Let \mathcal{G} be the set of ground-truth object names and \mathcal{P} the set of predicted names; the intersection $\mathcal{M} = \mathcal{G} \cap \mathcal{P}$ defines matched objects, while $\mathcal{G} \setminus \mathcal{P}$ are missed. For every $o \in \mathcal{M}$, we compute:

- the IoU between the predicted and ground-truth boxes, $\text{IoU}_o = \text{IoU}(\hat{B}_o, B_o^*)$ in ratio space; and
- the absolute depth error, $|\hat{d}_o - d_o^*|$, where both depths are in $[0, 1]$.

At the example level, we record: (i) the number of ground-truth objects $|\mathcal{G}|$; (ii) the number of missed objects $|\mathcal{G} \setminus \mathcal{P}|$; (iii) the mean IoU over matched objects; and (iv) the mean absolute depth error over matched objects. Aggregating over the entire benchmark yields:

- the *grounded ratio*, defined as $1 - \frac{\sum_{\text{missed}}}{\sum |\mathcal{G}|}$, i.e., the fraction of ground-truth objects that are explicitly grounded by the model;
- the overall mean IoU across all matched objects; and
- the overall mean absolute depth error across all matched objects.

These metrics jointly capture whether models (i) choose to ground the right objects in their reasoning, (ii) localize them precisely in 2D, and (iii) assign consistent ordinal depths. Since the protocol never prescribes *which* objects must be grounded in advance, high scores indicate that spatial grounding emerges naturally as part of the model’s reasoning process, rather than being enforced by the evaluation interface.

11. Prompts Design

We provide the prompts used in dataset generation and GPT-evaluation in Fig. 7, Fig. 8, Fig. 9, Fig. 10, Fig. 11, Fig. 12, Fig. 13, Fig. 14, Fig. 15.

12. More Data Examples

We show more examples in our dataset in Fig. 16, Fig. 17, Fig. 18, and Fig. 19.

13. More inference Examples

We provide more inference examples in Fig. 20, Fig. 21, and Fig. 22

```

You are a helpful assistant.

# Tools
You may call one or more functions to assist with the user query.
You are provided with function signatures within <tools></tools> XML tags:
<tools>
{"type":"function",
 "function":{
  "name":"image_zoom_in_tool",
  "description":"Zoom in on a specific region of an image by cropping it based on a
    RATIO-BASED bounding box (bbox_2d). IMPORTANT: All coordinates must be ratios
    between 0 and 1, not absolute pixel values.",
  "parameters":{
    "properties":{
      "bbox_2d":{
        "type":"array",
        "items":{"type":"number"},
        "minItems":4,
        "maxItems":4,
        "description":"The bounding box of the region to zoom in, as [x1,y1,x2,y2],
          where (x1,y1) is the top-left corner and (x2,y2) is the bottom-right. All
          values MUST be ratios between 0 and 1."
      }
    },
    "required":["bbox_2d"],
    "type":"object"
  },
  "args_format":"Format the arguments as a JSON object."
}}
</tools>

## STRICT FORMATTING
- Always wrap private reasoning in <think>...</think>.
- If zooming: output EXACTLY ONE <tool_call>...</tool_call>.
- If NOT zooming: output BOTH <think>...</think> and <answer>...</answer>.
- Never mix <answer> with <tool_call>.
- Output nothing outside these tags.

## DECISION RULE (when to call the tool)
Call the zoom tool ONLY IF at least one is true:
1) The target text/object is too small or low-resolution.
2) Counting/attribute verification requires isolating a region.
3) Multiple candidate regions exist and must be disambiguated.

Do NOT call the tool when:
- The answer is already visible.
- The question is answerable from global context.
- Additional pixels would not give new information.

## OUTPUT STYLE
- Be concise and answer exactly the question.
- Never mix <answer> with <tool_call>.

```

Figure 7. System prompt used for 2D VisReason generation. The model decides whether zoom-in is needed and must follow strict XML-style reasoning and tool usage rules.

```

Answer the question by first thinking.

If a tighter crop is required, call image_zoom_in_tool once.
If the current view is sufficient, produce <think>...</think>
followed immediately by <answer>...</answer>.

Formatting (must follow strictly):
- Always include <think>...</think>.
- If zooming: output exactly one <tool_call>...</tool_call>.
- If NOT zooming: output <think>...</think> + <answer>...</answer>.
- Never mix <answer> with <tool_call>.
- Output nothing outside these tags.

```

Figure 8. First-round prompt for VisReason. The model must decide whether the full image is sufficient or whether zooming is required.

```

Think first. If a tighter crop is required, call image_zoom_in_tool
ON THE CURRENT VIEW (result of previous crop).

If the area is already sufficient, produce reasoning + final answer.

Formatting:
- Always include <think>...</think>.
- If zooming: EXACTLY ONE <tool_call>...</tool_call>.
- If NOT zooming: <think>...</think> + <answer>...</answer>.
- Never mix <answer> with <tool_call>.

```

Figure 9. Later-round prompt for VisReason. The model continues zoom-in refinement only when necessary.

```

You are given:
- An image showing a complex scene.
- A list of all objects in the image (objects_ratio).
  Each object includes its category, bounding box [x1,y1,x2,y2],
  and its depth value.

Your task is:
1. Provide a natural scene description.
2. Predict an Area of Interest (AoI) formatted as [x1,y1,x2,y2] in [0,1].
  The AoI must:
  - Strictly cover the object(s) relevant to the question;
  - Include necessary context;
  - Avoid unrelated areas.
3. Provide a brief reasoning step explaining why this area is sufficient.

Output format:

Scene Description:
[your description]

Area of Interest:
[x1, y1, x2, y2]

Reasoning:
[your explanation]

```

Figure 10. Prompt used for first-round full-image RoI generation in 2D VisReason.

You are given an image with:

- A list of objects {category, bounding box [x1,y1,x2,y2], depth value};
- Monocular depth map + segmentation-derived object ordering.

Your task:

Generate a 3D-aware question-answer pair (q, a, B*) that:

- Combines 2D relations (left of, right of, above, below) WITH depth relations (in front of, behind);
- Identifies a single target object and produces its GT box B*;
- Avoids ambiguous or underspecified relations;
- Produces a question solvable from the image alone.

Figure 11. Prompt for generating 3D-aware QA pairs used in VisReason-Pro construction.

Given: image crop, question q, answer a, and local object list O_t.

Each object includes:

- category,
- bounding box [x1,y1,x2,y2],
- ordinal depth.

Task:

1. Provide a concise scene description based on the CURRENT CROP.
2. Predict an area of interest (AoI) [x1,y1,x2,y2] in [0,1].
3. Provide a brief reasoning step.

Rules:

- AoI must cover the target object and supporting evidence.
- Use depth information to disambiguate occlusions or ordering.
- Use <think> for reasoning and <answer> for explanation.

Figure 12. 3D-aware CoT step prompt used in VisReason-Pro for each zoom-in round.

Given multi-round traces {desc_t, AoI_t, reason_t}, distill them into a SINGLE compact reasoning step:

- Summarize the multi-round logic into one brief explanation.
- Output ONE final AoI box in ratio coordinates [x1,y1,x2,y2].
- Ensure the box tightly covers the correct target object.
- Avoid mentioning intermediate zooms, crops, or recursion.

Figure 13. Prompt for single-round distillation in VisReason-Pro. Converts multi-round chains into a compact one-shot explanation.

You are given a piece of reasoning text and a list of visible objects with grounding annotations.

Visible objects (JSON):
{objects_json}

Task:

- Rewrite the reasoning text by inserting grounding right AFTER each mentioned key object.
- Grounding format: object_name ([x1, y1, x2, y2], depth_value).
- If depth_value is null or missing, output only ([x1, y1, x2, y2]).
- DO NOT change wording or add new information. Preserve the original reasoning flow.
- DO NOT add objects that are not mentioned.
- Return only the rewritten text.

Text:

{base_text}

Figure 14. Prompt for grounding augmentation during VISREASON-PRO generation. The model rewrites the reasoning text by inserting explicit spatial grounding ([x1, y1, x2, y2], depth) after each referenced object without altering the semantic content.

You are an automatic grader. Given Question / Standard answer / Model's answer, output a similarity score in [0,1] and nothing else, formatted exactly as: score: <score> (up to two decimals).

Rules:

- Normalize case and whitespace before comparing.
- Unify number and time formats when they are semantically equivalent.
- If the model answer is exactly the same as the standard answer (or only differs in trivial formatting), output score: 1.00.
- If the two answers are synonyms or one clearly contains the other without contradiction, output a score in the range 0.95-1.00.
- If there are minor wording differences but the core meaning is the same, use a score around 0.85-0.94.
- If there is only partial overlap in meaning, use a score around 0.75-0.84.
- If the answer is unrelated, contradictory, or clearly wrong, use a score close to 0.00.

For numerical answers:

- Use smaller relative error for higher scores.
 - If both are intervals, use larger overlap for higher scores.
- Grade only the core answer, ignoring polite phrases or extra commentary.

Figure 15. Prompt used for GPT-based similarity grading. The grader receives the question, standard answer, and model prediction, and returns a single scalar score in [0, 1] following the specified rubric.



Figure 16. More data examples in VisReason.

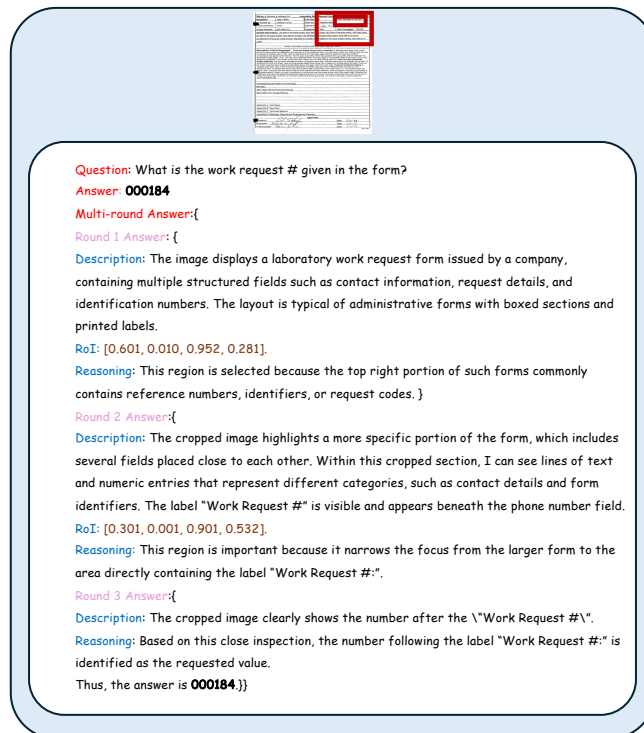


Figure 17. More data examples in VisReason.



Question: What is the person doing?

Answer: **Sitting on a seesaw**

Multi-round Answer:{

Round 1 Answer: {

Description: The image shows what at first appears to be a teddy bear placed on a wooden bench, but upon closer inspection, it seems to be part of a larger outdoor scene. The background resembles a park or playground setting, with natural light and surrounding greenery.

RoI: [0.000, 0.119, 0.312, 0.378].

Reasoning: This area is chosen because it contains shapes and textures that resemble a person's outline rather than just background elements. Although the initial impression is ambiguous, it is the most likely region to include the subject of interest.

Round 2 Answer:{

Description: The cropped image reveals a person dressed in red clothing. The figure is no longer confused with surrounding objects, and the structure of the playground equipment becomes visible in this view.

Reasoning: I can clearly recognize the person's activity. The body posture indicates that the individual is sitting on a seesaw. Thus, the answer is: **the person is sitting on a seesaw.** }}

Figure 18. More data examples in VisReason.



Question: What is the man wearing green jacket holding in his hands?

Answer: **A cup and its tray**

Multi-round Answer:{

Round 1 Answer: {

Description: The image shows a group of three people, consisting of two men and one woman, seated next to each other in what looks like a casual indoor setting. The man in the green jacket is positioned in the left, leaning slightly towards the woman as if engaged in a conversation. Meanwhile, the other man is seated nearby, focusing on his laptop which rests on his lap.

RoI: [0.317,0.000,0.579,0.812].

Reasoning: This region is chosen because it isolates the man in the green jacket, who is the subject of the question.

Round 2 Answer:{

Description: The cropped image provides a closer look at the man in the green jacket. He is wearing a black hat. His upper body and arm positions become clearer in this cropped view.

RoI: [0.213,0.342,0.712,0.609].

Reasoning: This region contains the man's hands, where I can find what he is holding.

Round 3 Answer:{

Description: The cropped image now focuses closely on the man's hands. He is holding a cup in one hand, and in his other hand, he supports a tray.

Reasoning: It is evident that the man is holding a cup along with a tray. Thus, the answer is **"cup and tray"** }}

Figure 19. More data examples in VisReason.

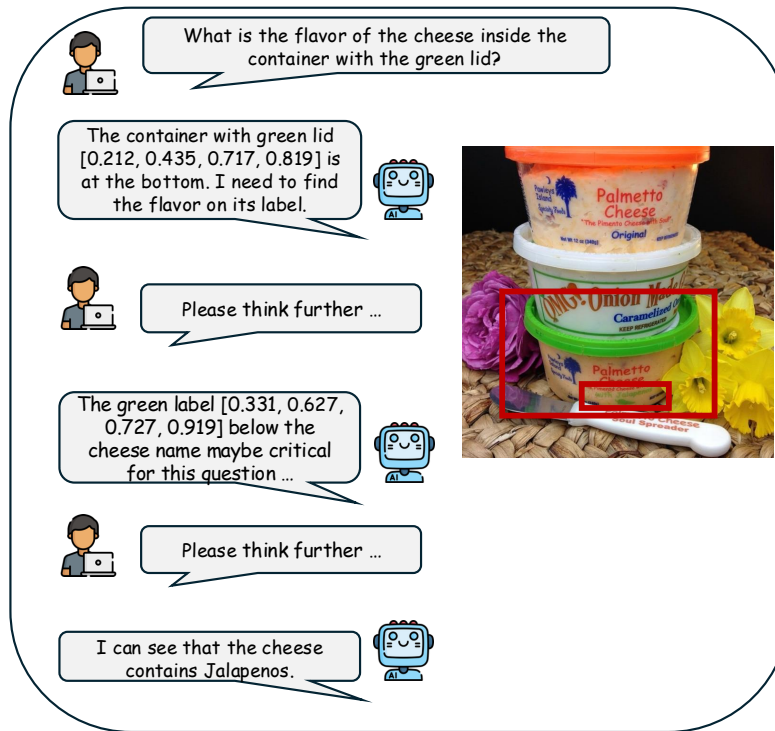


Figure 20. More inference examples in **VisReason**.

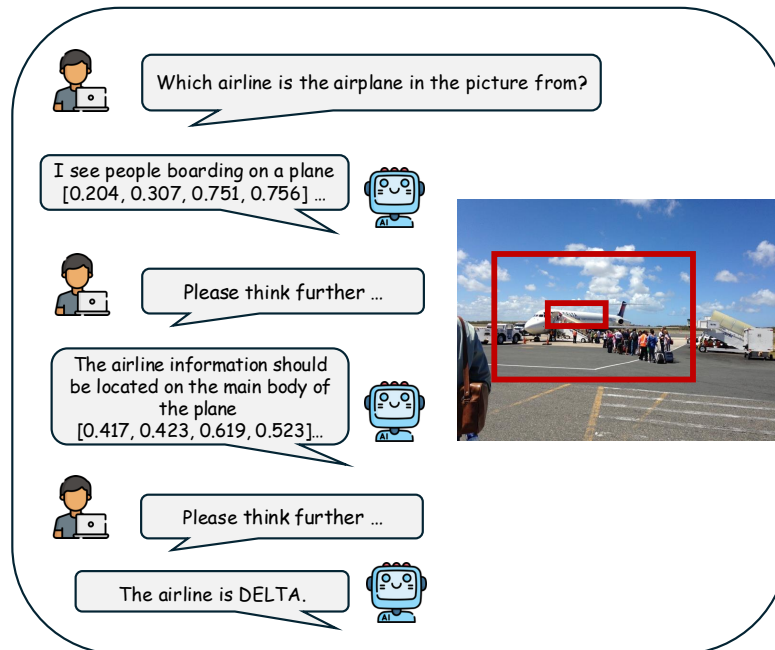


Figure 21. More inference examples in **VisReason**.

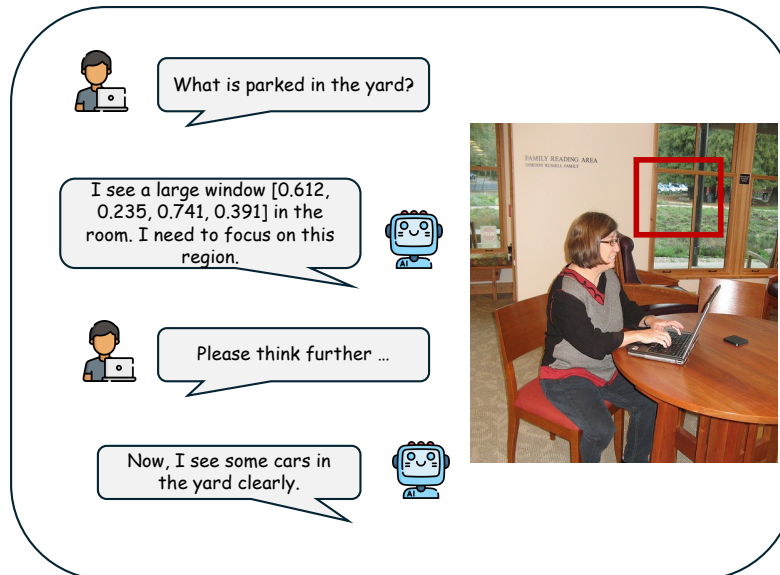


Figure 22. More inference examples in **VisReason**.